



Dissipation and dilatation rates in premixed turbulent flames

Downloaded from: <https://research.chalmers.se>, 2026-04-05 19:05 UTC

Citation for the original published paper (version of record):

Sabelnikov, V., Lipatnikov, A., Nishiki, S. et al (2021). Dissipation and dilatation rates in premixed turbulent flames. *Physics of Fluids*, 33(3). <http://dx.doi.org/10.1063/5.0039101>

N.B. When citing this work, cite the original published paper.

Dissipation and dilatation

1 Dissipation and dilatation rates in premixed turbulent flames

2 V. A. Sabelnikov,^{1, a)} A. N. Lipatnikov,² S. Nishiki,³ H. L. Dave,⁴ F. E. Hernández Pérez,⁵ W. Song,⁵ and Hong G. Im⁵

3 ¹⁾Central Aerohydrodynamic Institute (TsAGI), 140180 Zhukovsky, Moscow Region, Russian Federation ^{b)}

4 ²⁾Department of Mechanics and Maritime Sciences, Chalmers University of Technology, Göteborg, 412 96, Sweden

5 ³⁾Department of Information and Electronic Engineering, Teikyo University, Utsunomiya 320-8551, Japan

6 ⁴⁾Department of Aerospace Engineering, Indian Institute of Science (IISc), Bengaluru, 560012, India

7 ⁵⁾Clean Combustion Research Center, King Abdullah University of Science and Technology, Thuwal 23955-6900, Saudi Arabia

8
9
10
11
12

13 (Dated: 7 January 2021)

14 Velocity dilatation, as well as total, solenoidal, and dilatational dissipation rates of the total flow kinetic energy are extracted from three different direct numerical simulation databases obtained by three independent research groups using different numerical codes and methods (e.g., single-step chemistry and complex chemistry flames) from six different premixed turbulent flames associated with flamelet, thin reaction zone, and broken reaction zone regimes of turbulent burning. Results show that dilatational dissipation can be larger than solenoidal dissipation in the flamelet regime and is substantial in the thin reaction zone regime. Accordingly, the influence of combustion-induced thermal expansion on dissipation rate is not reduced to an increase in the mixture viscosity by the temperature. A simple criterion for identifying conditions associated with significant dilatational dissipation is discussed and dilatational dissipation due to the influence of turbulence on mixing in preheat zones is argued to play a role even at high Karlovitz numbers Ka . In particular, the magnitude of dilatation fluctuations and probability of finding negative local dilatation are increased by Ka , thus, implying that the impact of molecular transport of species and heat on the dilatation increases with increasing Karlovitz number.

15
16
17
18
19
20
21
22
23
24
25
26 PACS numbers: 47.70.Fw, 82.33.Vx, 47.27.-i

27 Keywords: dissipation rate, solenoidal dissipation, dilatational dissipation, premixed turbulent combustion, thermal expansion, DNS

29 I. INTRODUCTION

30 The mean rate $\overline{\rho\epsilon}$ of viscous dissipation of kinetic energy of a turbulent flow (or dissipation rate for brevity) is one of the most important quantities in the turbulence theory.¹⁻⁶ The dissipation rate is defined as follows:

$$34 \quad \overline{\rho\epsilon} \equiv \overline{\tau_{ij}S_{ij}}, \quad (1)$$

35 where

$$36 \quad \tau_{ij} = 2\mu \left(S_{ij} - \frac{1}{3}\delta_{ij}\frac{\partial u_k}{\partial x_k} \right) + \mu_v \delta_{ij}\frac{\partial u_k}{\partial x_k} \quad (2)$$

37 is the viscous stress tensor, $S_{ij} = (\partial u_i/\partial x_j + \partial u_j/\partial x_i)/2$ is the strain rate tensor, μ is the dynamic viscosity, μ_v is the bulk viscosity, u_i is the i -th component of the velocity vector \mathbf{u} , and δ_{ij} is the Kronecker delta, with the summation convention applying to repeated indexes. If $\mu_v = 0$, the dissipation rate can be decomposed as follows:⁷⁻¹¹

$$43 \quad \overline{\rho\epsilon} = \overline{\mu\omega^2} + \frac{4}{3}\overline{\mu\Theta^2} + 2\overline{\mu\frac{\partial^2}{\partial x_i\partial x_j}(u_i u_j)} - 4\overline{\mu\frac{\partial}{\partial x_i}(u_i\Theta)}, \quad (3)$$

44 where $\omega^2 = \omega_k\omega_k$ is the enstrophy, $\omega_i = \epsilon_{ijk}\partial u_j/\partial x_k$ is the i -th component of the vorticity vector, $\Theta = \partial u_k/\partial x_k$ designates dilatation, and ϵ_{ijk} is the cyclic permutation tensor. The first and second terms on the right hand side (RHS) of Eq. (3) are known as solenoidal and dilatational dissipation,⁷ respectively, whereas the third and fourth terms are mixed terms, i.e. they contain contributions from both solenoidal and dilatational velocity components. In the following, these two mixed terms will be considered jointly. If the viscosity μ is constant, the mixed terms asymptotically vanish at high Reynolds numbers because they contain spatial derivatives of mean quantities, whereas the solenoidal and dilatational dissipations involve mean values of squares of local spatial derivatives. For the same reason, dissipation rates evaluated using total or fluctuating velocity fields are asymptotically equal to one another at high Reynolds numbers.

45
46
47
48
49
50
51
52
53
54
55
56
57
58
59
60
61
62
63
64
65
66
67 In incompressible turbulent flows, dilatation vanishes and the dissipation rate is asymptotically equal to the solenoidal dissipation at high Reynolds numbers. If density varies due to pressure variations in high-speed flows, heat release at almost constant pressure in low-speed reacting flows, or both pressure variations and heat release (e.g., combustion in supersonic flows), dilatational dissipation plays a role. For instance, in high-speed non-reacting flows, a ratio

$$\chi = \frac{4}{3}\frac{\overline{\Theta^2}}{\overline{\omega^2}} \quad (4)$$

^{a)}Electronic mail: sabelnikov@free.fr.

^{b)}Also at ONERA - The French Aerospace Lab., F-91761 Palaiseau, France

This is the author's peer reviewed, accepted manuscript. However, the online version of record will be different from this version once it has been copyedited and typeset.

PLEASE CITE THIS ARTICLE AS DOI: 10.1063/1.50039101

of dilatational and solenoidal dissipations was reported^{7,12} scale as αM_t^2 in a first approximation, with the factor α being substantially less than unity. Here, $M_t = u'/C$ is the turbulence Mach number, u' is the root-mean-square (rms) velocity, and C is a representative speed of sound. In subsequent studies of compressibility effects on turbulence characteristics (spectra, a ratio of dilatational kinetic energy to solenoidal kinetic energy, a ratio of dilatational dissipation to solenoidal dissipation, etc.) in homogeneous non-reacting flows,^{13–18} dependence of the ratio χ on M_t was clarified, e.g. $\chi \propto M_t^4$ at $M_t < 0.4$,¹⁶ with substantial dependence of χ on the turbulent Reynolds number $Re_\lambda = u'\lambda/\nu$ being also documented, as reviewed elsewhere.¹⁷ Here, λ is the Taylor length scale and $\nu = \mu/\rho$ is the kinematic viscosity of the fluid.

Recently, Donzis and John¹⁷ have analyzed a large set of published and their own direct numerical simulation (DNS) data and have shown that the ratio χ is proportional to a ratio of dilatational and solenoidal turbulent kinetic energies, k_d/k_s , and k_s , respectively, with these two ratios varying by almost ten and five orders of magnitude, respectively. When the same data are plotted vs. M_t , the scatter of the data is significantly more pronounced. More specifically, at $M_t < 0.2$, DNS data generated by Donzis and John¹⁷ using either solenoidal or dilatational forcing differ drastically from one another, i.e., the ratio χ can be as large as 10^3 in the latter case, whereas $\chi \ll 1$ in the former case (if $M_t < 0.2$). An important role played by the ratio of k_d/k_s was also revealed in a recent study of compressibility effects in mixing of passive scalars in homogeneous flows.¹⁸

In subsonic reacting flows, non-negligible values of the ratio χ were found in non-premixed flames with homogeneous initial conditions at $0 < Ma_t < 0.5$ ^{19–22} and in a spatially developing shear layer at $Ma_t \ll 1$.²³ In all these studies, χ was significantly less than unity. Recently, Teng et al.¹⁶ numerically explored evolution of initially unmixed reacting flows embedded into homogeneous isotropic turbulence. The obtained DNS data show that the ratio χ depends substantially on a heat release parameter (a ratio of the heat of reaction to a reference enthalpy in the cited paper) and a Damköhler number Da , which characterizes a ratio of the turbulence reaction time scales, whereas the dependence of χ on Re_λ is weakly pronounced at high Da . Under conditions of the discussed DNS, the ratio χ can be larger than unity if $M_t = 0.6$ and the Damköhler number is as large as 3000. However, the computed χ is significantly less than unity for $M_t = 0.2$ even if $Da = 3000$.

Accordingly, to the leading order, the influence of reaction induced density variations on the dissipation rate may be summed to be controlled by an increase in the solenoidal dissipation due to an increase in the viscosity with the temperature in reacting flows characterized by a low Mach number.^{16,20–22} Contrary to the aforementioned studies of the influence of heat release on dissipation rate in the non-premixed mode of turbulent burning, the present authors are not aware of evaluation of the ratio χ in premixed flames (note that such a flame is characterized by significant spatial gradient of the mean flow velocity in the direction normal to the mean flame surface). Nevertheless, in a recent DNS study^{24,25} of highly turbulent

premixed flames, the influence of combustion-induced thermal expansion on small-scale turbulence was also attributed to the increase in the mixture viscosity.

Based on the recent findings by Donzis and John,¹⁷ John et al.,¹⁸ and Teng et al.,¹⁶ one may hypothesize that, in premixed turbulent flames characterized by $M_t \ll 1$, the ratio χ depends on Re_λ , k_d/k_s , the density ratio $\sigma = \rho_u/\rho_b$, and Da (note that the Karlovitz number defined later is proportional to Re_λ/Da in premixed flames). In other words, if $M_t \ll 1$,

$$\chi = f(Re_\lambda, k_d/k_s, \sigma, Da), \quad (5)$$

where f is a “universal” non-dimensional function. To our knowledge, there are neither theories nor numerical data on the dependence of the ratio χ on the aforementioned non-dimensional parameters. On the contrary, as reviewed elsewhere,^{26,27} numerical modeling of premixed turbulent combustion relies commonly on theories and models of constant-density turbulence characterized by $\nabla \cdot \mathbf{u} = 0$ and vanishing dilatational dissipation. Since dissipation rate plays a key role in the turbulence theory,^{1–6} eventual change of the physical nature of dissipation in premixed flames when compared to constant-density turbulence, i.e. appearance of dilatational dissipation in the former case, requires thorough investigation and, in particular, evaluation of the ratio χ in the case of premixed turbulent burning.

Accordingly, the major goals of the present study are (i) to examine dilatation in premixed turbulent flames characterized by a very low Mach number and various (small, moderate, and high) Karlovitz numbers and (ii) to demonstrate that dilatational dissipation can play a substantial role in such flames. For this purpose, three DNS databases that are described briefly in the next section were analyzed. Results are reported and discussed in the third section, followed by conclusions.

II. DNS ATTRIBUTES

Analyzed in the present work are the following three DNS databases: (i) Nagoya data that were created by Nishiki et al.^{28,29} about 20 years ago and were subsequently explored by various research groups,^{30–34} (ii) Bangalore data that were computed recently by Dave and Chaudhuri⁵⁵ and were subsequently analyzed by two of the present authors,^{56,57} and (iii) KAUST data^{58–60} that were also used by various research groups.^{61–64} In the following, major attributes of these three DNS series are briefly summarized. The reader interested in more details is referred to the cited papers.

All these unsteady three-dimensional simulations had certain common features. First, they addressed statistically planar and one-dimensional, adiabatic premixed flames propagating in rectangular channels. Second, the governing equations were solved in compressible form. Third, homogeneous isotropic turbulence was generated in a separate box, was injected into the computational domain through the left boundary $x = 0$ and decayed along the direction x of the mean flow. Fourth, the simulated flows were periodic in y and z directions. Fifth, a planar laminar flame was embedded into tur-

This is the author's peer reviewed, accepted manuscript. However, the online version of record will be different from this version once it has been copyedited and typeset.

PLEASE CITE THIS ARTICLE AS DOI: 10.1063/5.0039101

181 bulent flow in the computational domain at $t = 0$. Subse-
182 quently, the mean inflow velocity was changed twice^{28,29} or
183 gradually^{55,58-60} to match turbulent flame speed. Sixth, in the
184 present paper, the combustion progress variable is defined as
185 follows

$$c = \frac{T - T_u}{T_b - T_u}, \quad (6)$$

187 where T is the temperature and subscripts u and b designate²³⁰
188 unburned reactants and burned products, respectively. ²³²

189 Major characteristics of the simulated flames are reported
190 in Table I. Here, S_L and $\delta_L = (T_b - T_u) / \max |\nabla T|$ are the lam-²³³
191 inar flame speed and thickness, respectively, $\sigma = \rho_u / \rho_b$ is the²³⁴
192 density ratio, u' and L are the rms velocity and an integra-²³⁵
193 length scale, respectively, of turbulence generated in a box²³⁶
194 $\tau_t = L / u'$ is the eddy-turn-over time, $Re_t = u' L / \nu_u$ is the tur-
195 bulent Reynolds number, $Ka = (u' / S_L)^2 Re_t^{-1/2} (S_L \delta_L / \nu_u)$ is
196 the Karlovitz number, and ν_u is the kinematic viscosity of un-
197 burned mixture. The Karlovitz number is proportional to a
198 ratio of the flame time scale $\tau_f = \delta_L / S_L$ to the Kolmogorov
199 time scale $\tau_K = (\nu_u / \bar{\epsilon})^{1/2}$, with the coefficient of proportion²³⁷
200 $\sqrt{C_d}$ being of unity order if $\bar{\epsilon} = C_d u'^3 / L$.^{2,5} Certain spec-
201 ific features of the discussed DNS databases are noted in the
202 following subsections.

203 A. Nagoya DNS database

204 A computational domain of $8 \times 4 \times 4$ mm was resolved us-
205 ing a uniform rectangular ($2\Delta x = \Delta y = \Delta z$) mesh of $512 \times$
206 128×128 points. ²⁴⁵

207 Combustion chemistry was reduced to a single reaction, the²⁴⁶
208 Lewis and Prandtl numbers were equal to 1.0 and 0.7, re-²⁴⁷
209 spectively, and the mixture state was completely characterized²⁴⁸
210 with a single combustion progress variable c . Temperature²⁴⁹
211 dependence of molecular transport coefficients was taken into²⁵⁰
212 account, e.g., $\nu = \nu_u (T / T_u)^{1.7}$. ²⁵¹

213 Flames H and L are characterized by high and low density²⁵²
214 ratios, respectively, with all other parameters being approxi-
215 mately equal (the first and second lines, respectively, in Table²⁵³
216 I). These flames are well associated with the flamelet combus-²⁵⁴
217 tion regime,⁶⁵ as shown elsewhere.³⁷ ²⁵⁵

218 Results reported in the following were averaged over trans-²⁵⁶
219 verse planes and a time interval of $1.5\tau_t$, associated with fully²⁵⁷
220 developed flames, as discussed in detail elsewhere.⁵¹ ²⁵⁸

221 B. Bangalore DNS database

222 The DNS data were computed adopting the Pencil code.⁶⁶ ²⁶³
223 A computational domain of $19.18 \times 4.8 \times 4.8$ mm was dis-²⁶⁴
224 cretized using a uniform mesh of $960 \times 240 \times 240$ nodes. ²⁶⁵

225 A lean (the equivalence ratio $\Phi = 0.81$) and slightly pre-²⁶⁶
226 heated ($T_u = 310$ K) hydrogen-air flame was studied using ²⁶⁷
227 detailed reaction mechanism (9 species, 21 reactions) by Li et al.²⁶⁸
228 al.⁶⁷ and mixture-averaged transport coefficients, which de-²⁶⁹
229 pended on temperature. The simulation conditions (flame IIS⁷⁰

FIG. 1. Dissipation rate normalized using $\mu_u S_L^2 / \delta_L^2$ and various con-
tributions to it vs. Reynolds-averaged combustion progress variable
 \bar{c} . (a) Nagoya flame H, (b) Nagoya flame L, (c) Bangalore flame IIS,
(d) KAUST flame A, (e) KAUST flame B, (f) KAUST flame C.

in the third line in Table I, where IIS is an abbreviation of In-
dian Institute of Science) are associated with the thin reaction
zone regime⁶⁵ of turbulent burning.

As discussed in detail elsewhere,^{56,57} results reported in the
following were averaged over transverse planes and various
instants (54 snapshots stored each $5 \mu\text{s}$ over the time period
 $1.401 \text{ ms} \leq t \leq 1.566 \text{ ms}$).

C. KAUST DNS database

In cases A and B, a computational domain of $20 \times 10 \times 10$
mm was discretized using a uniform mesh of $512 \times 256 \times$
 256 nodes, whereas in case C, a computational domain of
 $8.32 \times 2.08 \times 2.08$ mm was discretized using a uniform mesh
of $1280 \times 320 \times 320$ nodes. To solve the governing equations,
an eighth-order central difference and an explicit fourth-order
Runge-Kutta schemes were employed.⁵⁸

A lean ($\Phi = 0.70$) hydrogen-air flame ($T_u = 300$ K) was
studied using a detailed reaction mechanism (9 species, 19
reactions) by Burke et al.⁶⁸ and mixture-averaged transport
coefficients, which depended on temperature. The simulation
conditions (the three bottom lines in Table I) are associated
with flamelet, thin reaction zone, and broken reaction zone
regimes⁶⁵ of turbulent burning in cases A, B, and C, respec-
tively.

As discussed in detail elsewhere,⁶³ results reported in the
following were averaged over transverse planes and six differ-
ent instants in each case, i.e., at $t/\tau_t = 0.57, 0.67, 0.77,$
 $0.86, 0.96,$ and 1.05 in case A and at $t/\tau_t = 4.1, 4.8, 5.5, 6.2,$
 $6.8,$ and 7.5 in cases B and C.

Since the major characteristics of the Nagoya flame H and
the KAUST flame A are similar and both flames are associated
with flamelet combustion regime, comparison of results com-
puted in these two cases allows us to examine the influence
of combustion chemistry and diffusive-thermal effects⁶⁹⁻⁷¹ on
the dissipation rate. Comparison of results obtained from the
Bangalore flame IIS and the KAUST flame B, which both
have similar major characteristics and are associated with thin
reaction zone regime of turbulent burning, allows us to check
the consistency of the two databases. Moreover, comparison
of results obtained from the KAUST flames A, B, and C al-
lows us to explore the influence of Karlovitz number on the
relation between the dilatational and solenoidal dissipations.

This is the author's peer reviewed, accepted manuscript. However, the online version of record will be different from this version once it has been copyedited and typeset.

PLEASE CITE THIS ARTICLE AS DOI: 10.1063/1.50039101

TABLE I. Characteristic parameters of DNS cases

Flame	S_L , m/s	δ_L , mm	σ	u' , m/s	L , mm	τ_r , ms	Re_t	Ka	$Ka/(\sigma - 1)$	M_t
H	0.6	0.217	7.53	0.53	3.5	6.6	96	0.60	0.09	0.0015
L	0.416	0.158	2.50	0.53	3.5	6.6	96	0.64	0.43	0.0015
IIS	1.84	0.36	6.15	6.7	3.1	0.46	950	19.0	3.7	0.02
A	1.36	0.36	5.95	0.95	5.0	5.3	227	0.75	0.15	0.002
B	1.36	0.36	5.95	6.8	5.0	0.74	1623	14.4	2.91	0.02
C	1.36	0.36	5.95	19.0	1.4	0.076	1298	126	25.5	0.055

271 III. RESULTS AND DISCUSSION

272 A. Comparison of solenoidal and dilatational dissipations

273 Figure 1 shows the total (solid lines), solenoidal (dashed) 274 lines), and dilatational (dotted-dashed lines) dissipations ex- 275 tracted from the six DNS data sets, as well as the sum (double- 276 dashed-dotted lines) of the last two terms on the RHS of Eq. 277 (3), referred to as ‘‘mixed.’’ The following trends are worth 278 noting.

279 First, in all six cases the sum of the last two terms on the 280 RHS of Eq. (3), whether it is positive or negative, is signifi- 281 cantly less than the total dissipation, including flames H and L 282 for which the turbulent Reynolds number is rather small (Figs. 283 1a and 1b).

284 Second, for flames H, L, and A in the flamelet combus- 285 tion regime, the dilatational dissipation can be larger than the 286 solenoidal dissipation. In flame H, characterized by a low Ka 287 and a high density ratio, the ratio χ defined by Eq. (4) is sig- 288 nificantly larger than unity in the entire flame brush, with the 289 exception of its trailing zone ($\bar{c} > 0.95$). In flame L, char- 290 acterized by a comparable Ka , but a significantly lower den- 291 sity ratio, the ratio χ is smaller (larger) than unity at $\bar{c} < 0.4$ 292 ($\bar{c} > 0.4$, respectively). This trend is attributed to decay of 293 the turbulence in the direction of the mean flow and a weak 294 (due to a low density ratio) influence of baroclinic torque on 295 vorticity within the L flame brush.³⁶ In flame H, such an in- 296 fluence is much stronger, as discussed in detail elsewhere.^{36,43} 297 In flame A characterized by a slightly higher (when com- 298 pared to flame H) Ka and a lower density ratio, the ratio χ 299 is smaller (larger) than unity at $\bar{c} > 0.4$ ($\bar{c} < 0.4$, respectively). 300 Differences in the behaviour of the ratio χ in flame A com- 301 pared to flames H/L stem not only from complex-chemistry³⁴⁶ 302 but also from diffusive-thermal effects, i.e. significant local³⁴⁷ 303 variations in the temperature and equivalence ratio due to im- 304 balance of heat and species fluxes from and to reaction zones³⁴⁸ 305 curved and strained by turbulent eddies. Such effects are well³⁴⁹ 306 known to play an important role in lean hydrogen-air turbulent³⁵⁰ 307 flames, as reviewed elsewhere,^{69–71} and, in particular, can sig-³⁵¹ 308 nificantly reduce local burning rate and combustion tempera-³⁵² 309 ture in negatively curved reaction zones. Since the probabil-³⁵³ 310 ity of finding such reaction zones is higher at large \bar{c} due to³⁵⁴ 311 purely topological reasoning, diffusive-thermal effects could³⁵⁵ 312 substantially reduce dilatational dissipation at large \bar{c} in lean³⁵⁶ 313 hydrogen-air turbulent flames.³⁵⁷

314 Third, even in flames IIS and B, characterized by $Ka > 10$ ³⁵⁸ 315 and associated with the thin reaction zone regime of premixed³⁵⁹

burning, differences between the total and solenoidal dissipa- 316 tions are significant, implying that the dilatational dissipation 317 is not negligible.

318 Fourth, in flame C, characterized by $Ka > 100$ and associ- 319 ated with the broken reaction zone regime of premixed turbu- 320 lent burning, the total dissipation is mainly controlled by the 321 solenoidal dissipation. This observation is consistent with re- 322 cent DNS data that were also obtained from highly turbulent 323 flames.^{24,25} Nevertheless, even in this case, dilatational dis- 324 sipation is substantial at $\bar{c} < 0.1$. Physical mechanisms that 325 could explain this observation will be discussed later. The 326 rapid decrease in $\overline{\rho\epsilon}$ with \bar{c} observed in Fig. 1f is attributed 327 to turbulence decay due to an increase in the mixture viscosity 328 with increasing temperature.

329 All in all, Fig. 1 shows that (i) dilatational dissipation 330 can play an important role even at low Mach numbers and 331 (ii) in the flamelet and thin reaction zone regimes of pre- 332 mixed burning, the influence of combustion-induced thermal 333 expansion on dissipation rate is not only due to an increase in 334 the mixture viscosity by the temperature, as commonly be- 335 lieved. Rather, the combustion-induced thermal expansion 336 changes the physical nature of the dissipation, shifting from 337 the dissipation of vortices in constant-density turbulence to 338 the dilatation-controlled dissipation in a premixed flame. Such 339 a fundamental change in the nature of the dissipation in pre- 340 mixed flames casts doubts on the direct application of conven- 341 tional constant-density turbulence models for simulations of 342 premixed combustion. Other phenomena associated with the 343 influence of combustion-induced thermal expansion on turbu- 344 lence in premixed flames are reviewed elsewhere.^{26,27}

345 B. A simple criterion to estimate importance of dilatational 346 dissipation

347 The simplest estimate of a criterion for indicating impor- 348 tance of dilatational dissipation can be obtained by compar- 349 ing the magnitude of dilatation in the unperturbed laminar 350 flame, i.e. $(\sigma - 1)S_L/\delta_L$, with the mean magnitude τ_K^{-1} of 351 velocity gradients generated by the smallest eddies. Accord- 352 ingly, dilatational dissipation is expected to play a minor role 353 if $Ka/(\sigma - 1)$ is significantly larger than unity. As reported in 354 Table I, these values are consistent with the results shown in 355 Fig. 1f. A similar criterion of importance of thermal expansion 356 effects in premixed turbulent flames was earlier proposed 357 by Bilger,⁷² but based on a different reasoning. Recent DNS 358 data by MacArt et al.^{73,74} are also consistent with such a cri-

This is the author's peer reviewed, accepted manuscript. However, the online version of record will be different from this version once it has been copyedited and typeset.

PLEASE CITE THIS ARTICLE AS DOI: 10.1063/5.0039101

360 terion, while dilatational and solenoidal dissipations are not
361 compared in the cited papers.

362 Nevertheless, the above simple criterion should be considered
363 with a few cautions. First, it compares a statistically
364 averaged turbulence characteristic, i.e. τ_K^{-1} , with dilatation
365 $(\sigma - 1)S_L/\delta_L$ in the local laminar flame. To be more consistent,
366 multiplication of the dilatation with a probability γ of
367 finding such local flames should be used when comparing dilatational
368 and solenoidal dissipations in a premixed turbulent flame.
369 Accordingly, $Ka/(\sigma - 1)$ should be compared with $\gamma < 1$, rather than unity.
370 Since the probability γ is likely to increase with increasing Ka in moderately
371 turbulent flames and to reach a plateau close to unity at $Ka \gg 1$ and $Da \ll 1$,⁷⁵
372 the actual quantitative criterion is expected to be more complicated.
373
374

375 Second, since combustion increases the mixture viscosity,
376 and hence τ_K , evaluation of this time scale at a temperature
377 higher than T_u , e.g. $(T_u + T_b)/2$, appears to be more consistent.
378 In such a case, $Ka/(\sigma - 1)$ should be compared with $\gamma[(1 + \sigma)/2]^{0.85}$
379 if $v = v_u(T/T_u)^{1.7}$. For typical values of σ , the factor of $\gamma[(1 + \sigma)/2]^{0.85}$
380 could be sufficiently close to unity in the vicinity of the boundary of the domain
381 of importance of dilatational dissipation, but further research into the
382 discussed criterion is definitely required.
383
384

385 Third, in premixed turbulent flames, dilatational dissipation can
386 result not only from heat release, but also from the influence of turbulence
387 on molecular mixing in the local flame zones characterized by a negligible
388 heat release rate. To illustrate such an effect in a simple manner, let us
389 consider the following low-Mach-number transport equation for the
390 temperature
391

$$391 \quad c_p \rho \frac{\partial T}{\partial t} + c_p \rho u_k \frac{\partial T}{\partial x_k} = c_p \frac{\partial}{\partial t} (\rho T) + c_p \frac{\partial}{\partial x_k} (\rho T u_k) \\ 392 \quad = - \frac{\partial J_{k,T}}{\partial x_k} + \dot{\omega}_T, \quad (7)$$

393 where c_p is the mixture heat capacity at constant pressure, $\dot{\omega}_T$
394 is the heat release rate, and the symbol $J_{k,T}$ designates the k -th
395 component of the flux vector J_T , which involves fluxes due to
396 molecular transport of heat and species. Using the ideal gas
397 state equation of $pW = \rho RT$ and considering the asymptotic
398 case of a low Mach number $M \ll 1$, which is typical for pre-
399 mixed flames,^{76,78} the product of ρT may be substituted with
400 $\rho T = \rho_u T_u [(W/W_u) + O(M^2)]$. Here, W is molecular weight
401 of the mixture and R is the universal gas constant. Accordingly,
402 Eq. (7) reads⁷⁸

$$403 \quad \Theta \equiv \frac{\partial u_k}{\partial x_k} = \frac{R}{c_p \rho_u} \left(- \frac{\partial J_{k,T}}{\partial x_k} + \dot{\omega}_T \right) \\ 404 \quad - \frac{1}{W_u} \left(\frac{\partial W}{\partial t} + u_k \frac{\partial W}{\partial x_k} \right). \quad (8)$$

405 Furthermore, variations in the molecular weight W are weak
406 in a typical premixed flame, where $W \approx W_u$ is controlled by
407 the molecular weight of N_2 to the leading order. Accordingly,
408 the ideal gas state equation is commonly simplified to
409 $\rho T = \rho_u T_u$ in the premixed combustion literature.⁷⁶⁻⁷⁸ In such a

FIG. 2. Typical 2D images of heat release rate expressed in W/m^3
(top row), normalized dilatation rate $\Theta/[(\sigma - 1)S_L/\delta_L]$ (middle row),
and normalized dilatational dissipation $4\mu\Theta^2/(3\mu_u S_L^2/\delta_L^2)$ (bottom
row, with the color scale being logarithmic) in the KAUST flames A
(left column), B (middle column), and C (right columns).

FIG. 3. Probability Density Functions $P(\Theta)$ for the local instantaneous
dilatation $\Theta(x, t)$ normalized using $(\sigma - 1)S_L/\delta_L$ and conditioned
to various values of the local instantaneous $c(x, t)$, specified in
legends. (a) Bangalore flame IIS, (b) KAUST flame A, (c) KAUST
flame B, (d) KAUST flame C.

a simplified case and if $J_T = -\rho \kappa c_p \nabla T$, Eq. (7) reads⁷⁹⁻⁸¹

$$\Theta = \frac{1}{\rho_u T_u c_p} \left[\frac{\partial}{\partial x_k} \left(\rho \kappa c_p \frac{\partial T}{\partial x_k} \right) + \dot{\omega}_T \right] \\ = \frac{\rho S_d}{\rho_u T_u} |\nabla T| = \frac{\rho (T_b - T_u)}{\rho_u T_u} S_d |\nabla c|, \quad (9)$$

where κ designates molecular heat diffusivity of the mixture
and $S_d \equiv [\nabla \cdot (\rho \kappa c_p \nabla T) + \dot{\omega}_T]/(\rho c_p |\nabla T|)$ is a displacement
speed⁷⁷ of the iso-surface $T(x, t) = \text{const}$.

Even if time and spatial derivatives of the pressure p and
molecular weight W are neglected in Eq. (9), this simplified
equation offers an opportunity to illustrate that the local
dilatation may be significantly affected by molecular fluxes
in preheat (and, to a lesser extent, in radical recombination)
zones associated with low reaction rates. Moreover, molecular
mixing in turbulent flows is known to be significantly affected
by turbulent eddies.² Accordingly, at small and large
 $c(x, t)$, the local dilatation could be controlled by turbulence
if it is sufficiently strong and the sign of Θ may be not only
positive, but also negative (contrary to unperturbed laminar
premixed flames where dilatation is always positive). Indeed,
in Eq. (9), the dilatation Θ is proportional to the displacement
speed S_d , with negative displacement speeds being well
documented in DNS studies of highly turbulent premixed
flames.^{55,82-87} Henceforth, dilatation that stems from the
influence of turbulent eddies on molecular mixing in zones
where the temperature field is non-uniform due to combustion
is called turbulence-controlled dilatation for brevity. Since
both this influence and the negative displacement speeds are
more pronounced in more intense turbulence, that dilatation
could play a substantial role even at a high Karlovitz number
and, in particular, could notably affect the dissipation rate.
Appearance of zones characterized by negative dilatation and
substantial dilatational dissipation is observed upstream of the
heat release zone in images plotted in Fig. 2 for the KAUST
flames B and, especially C. Certain DNS data that are consistent
with this hypothesis are presented in the next subsection.

C. Influence of Karlovitz number on dilatation

Figure 3 shows variations in the conditioned Probability
Density Function (PDF) $P(\Theta^*)$ with the local instantaneous

This is the author's peer reviewed, accepted manuscript. However, the online version of record will be different from this version once it has been copyedited and typeset.

PLEASE CITE THIS ARTICLE AS DOI: 10.1063/1.50039101

FIG. 4. Correlation coefficients $C_{a,b} = (\overline{ab} - \bar{a}\bar{b})/(\overline{a^2} \overline{b^2})^{1/2}$ between dilatation and (a) combustion progress variable c , (b) strain rate a_t , (c) heat release rate $\dot{\omega}_T/c_p$, and (d) the magnitude $|\nabla c|$ of the gradient of the combustion progress variable vs. Reynolds-averaged combustion progress variable \bar{c} . Abbreviation IIS refers to flame simulated in the Indian Institute of Science.

combustion progress variable $c(x,t)$ that the PDF is conditioned to. These PDFs have been sampled from the entire computational domains in the complex-chemistry cases, IIS, A, B, and C. Henceforth, the symbol Θ^* designates the local instantaneous dilatation rate $\Theta(x,t)$ normalized using $(\sigma - 1)S_L/\delta_L$. The following trends are worth noting.

First, the variations in $P(\Theta^*)$ with $c(x,t)$ are non-monotonic. That is, in the upstream region, as $c(x,t)$ increases from 0.1 to 0.3, the peak value of the normalized dilatation increases while the PDF distribution broadens (with an exception for case IIS). As $c(x,t)$ increases further from 0.3 to 0.7, the PDF distribution becomes narrower while the peak value decreases. This behavior is attributed to the fact that the dilatation and heat release rate peak in the interval $0.2 < c < 0.3$ in the unperturbed laminar flames associated with the Bangalore and KAUST simulations. Moreover, the monotonic attenuation in turbulence intensity leads to a narrower PDF distribution towards the downstream of the flame.

Second, as expected, the PDFs are wider in more intense turbulence, i.e. at higher Ka , cf. flames A, B, and C.

Third, while the probability of finding negative dilatation is low in flames IIS, A, and B, the PDF $P(\Theta^*)$ does not vanish at negative Θ^* in case C, thus indicating that the turbulence-controlled dilatation does play a role in flame C.

The role of turbulence-controlled dilatation at strong turbulence is further evidenced in Fig. 4, which reports various correlation coefficients $C_{a,b} = (\overline{ab} - \bar{a}\bar{b})/(\overline{a^2} \overline{b^2})^{1/2}$. In particular, Fig. 4a shows that, in flame H, L, IIS, A, or B, the correlation coefficient $C_{\Theta,c}$ between dilatation and combustion progress variable decreases monotonously with \bar{c} in the largest part of the mean flame brush with the exception of its trailing zones. This trend is associated with the fact that (i) appearance of the local flame in a point x close to the leading (trailing) edge of the mean flame brush causes a positive (negative) local fluctuation $c'(x,t)$ and (ii) combustion-induced dilatation is predominantly positive in these weakly and moderately turbulent flames. Accordingly, $C_{\Theta,c}$ is positive at $\bar{c} < c^*$ and negative at $\bar{c} > c^*$, with c^* being close to 0.5. However, such behaviour is not observed in the highly turbulent flame C, where $C_{\Theta,c}$ is close to zero at $\bar{c} < 0.3$, thus implying that other physical mechanisms (e.g. the influence of turbulence on molecular mixing) significantly affect dilatation in that zone. Moreover, in flame C, the coefficient $C_{\Theta,c}$ decreases at $\bar{c} > 0.3$ eventually due to the rapid decay of turbulence, as seen in Fig. 1f. Due to this rapid decay, the turbulence-controlled dilatation effect pronounced in flame C becomes mitigated at $\bar{c} > 0.3$.

Figure 4b shows that the correlation coefficient C_{Θ,a_t} between dilatation and the local strain rate $a_t = -n \cdot \nabla u$ is about 0.4-0.5 in the largest parts of the IIS, A, and

B flame brushes, as well as in flame C provided that $\bar{c} > 0.3$. Here, $n = -\nabla c/|\nabla c|$ designates the unit normal vector. This positive correlation is attributed to a decrease in the local flame thickness (and, hence, an increase in dilatation) in positively strained local flames. Such an effect is well known in the theory of strained laminar premixed flames⁸⁸ since the pioneering work by Klimov.⁸⁹ An increase in C_{Θ,a_t} with \bar{c} in the single-step-chemistry flames H and L is attributed to a more important role played by the local curvature (strain rate) at small (large, respectively) \bar{c} in these flames, as discussed elsewhere.⁴² However, in the leading zone ($\bar{c} < 0.3$) of flame C, the correlation coefficient is significantly lower than in other complex-chemistry flames, implying again that other physical mechanisms (e.g. the influence of turbulence on molecular mixing) significantly affect dilatation in that zone.

Figure 4c shows that the correlation coefficient C_{Θ,Ω_T} between dilatation and the local heat release rate $\Omega_T = \dot{\omega}_T/c_p$ is close to unity in the largest parts of the IIS, A, and B flame brushes with the exception of their trailing edges, as well as in flame C at $0.6 < \bar{c} < 0.85$. Such a strong correlation implies that the dilatation is mainly controlled by the combustion-induced thermal expansion in these complex-chemistry flames. In the leading zone of the C flame brush, however, the correlation coefficient is lower, again suggesting that other physical mechanisms (e.g. the influence of turbulence on molecular mixing) significantly affect dilatation in that zone. Note that, in the single-step-chemistry flames H and L, the coefficient C_{Θ,Ω_T} is lower, because dilatation and heat release rates peak at significantly different c (0.66 and 0.89, respectively) in the unperturbed laminar flames.

Figure 4d shows that the behaviour of the correlation coefficient $C_{\Theta,|\nabla c|}$ between dilatation and $|\nabla c|$ is similar to the behaviour of C_{Θ,Ω_T} , discussed above. The large value of $C_{\Theta,|\nabla c|}$ results directly from Eq. (9) that shows that $\Theta \propto |\nabla c|$. Lower values of $C_{\Theta,|\nabla c|}$ obtained in the leading zone of flame C indicate that the influence of turbulence on S_d (or, more specifically, on the molecular mixing term in the definition of S_d) plays an important role in that zone, in line with the above discussion of other results reported in Fig. 4. Moreover, these results reveal a way that flame propagation resists turbulent perturbations, an effect that, to our knowledge, has not yet been discussed in the literature. In other words, if turbulence strongly perturbs a flame locally and makes S_d negative in the flame preheat zone, the turbulence-controlled dilatation increases the local dissipation rate, thus mitigating the local turbulence.

Overall, the present DNS data (in particular, data obtained from flame C) indicate that the turbulence-controlled dilatation may play a role even in highly turbulent flames and, therefore, may notably contribute to the total dissipation rate. This issue definitely requires further DNS research into premixed turbulent flames characterized by Karlovitz numbers higher than the value of $Ka = 126$, which was reached in case C.

Note that if Ka is increased by decreasing the integral length scale L , the mean flame brush thickness δ_f may be decreased. Such an effect is evident in flame C when compared to flames A and B, as discussed elsewhere.⁶³ In particular, in case C, the time-averaged $\delta_f = 1/\max\{|\nabla \bar{c}|\}$ (i) is smaller by

FIG. 5. Mean dilatation $\nabla \cdot \bar{\mathbf{u}}$ normalized using $(\sigma - 1)S_L/\delta_L$ vs. Reynolds-averaged combustion progress variable.

FIG. 6. Magnitude $(\overline{\nabla \cdot \mathbf{u}'})^2$ of dilatation fluctuations, normalized using $(\sigma - 1)^2 S_L^2/\delta_L^2$, vs. Reynolds-averaged combustion progress variable.

555 a factor of about 3.5 than in case A or B and (ii) is approxi-
556 mately equal to $3\delta_L$. The decrease in δ_l results in increasing
557 the mean dilatation $\nabla \cdot \bar{\mathbf{u}}$. Indeed, Fig. 5 shows that $\nabla \cdot \bar{\mathbf{u}}$
558 is significantly larger in case C when compared to other five
559 cases.

560 Figure 6 shows that the magnitude $(\overline{\nabla \cdot \mathbf{u}'})^2$ of dilatation
561 fluctuations is significantly larger in flame C when compared
562 to other five cases. However, this difference is related more
563 to the turbulence-controlled dilatation rather than to the small
564 thickness δ_l of flame C.

565 D. Influence of diffusive-thermal effects on dilatation

566 When analyzing results plotted in Fig. 1f, one might at-
567 tribute substantial values of dilatational dissipation observed
568 at the leading edge of the mean C flame brush to diffusive-
569 thermal effects, which are discussed in detail elsewhere.
570 Such effects are well known to cause significant changes in
571 the local equivalence ratio and enthalpy (when compared to
572 the reference unperturbed laminar flame) due to imbalance of
573 local heat and species fluxes from/to reaction zones wrinkled
574 and strained by turbulent eddies. As a result, in lean hydrogen
575 air turbulent flames, local reaction rates, $|\nabla c|$, and combustion
576 temperature can be increased if the local flame curvature or
577 strain rate is positive.⁸⁸ Consequently, the local dilatation
578 also be increased.

579 Such effects are revealed in Fig. 7, which reports PDFs
580 $P(\Theta^*)$ of the normalized dilatation conditioned to various ra-
581 tios of $\Omega_T(x,t)/\max\{\Omega_T(x,t)\}$, with the maximum (over
582 the entire computational domain and various instants) heat
583 release rates $\max\{\Omega_T(x,t)\}$ being different due to differ-
584 ent magnitudes of the diffusive-thermal effects. More specifi-
585 cally, $\max\{\Omega_T(x,t)\}$ is significantly increased by Ka , i.e.
586 $\max\{\Omega_T(x,t)\} = 8600, 13\,500$ and $30\,000$ ($\text{g} \cdot \text{K}/(\text{cm}^3 \cdot \text{s})$) in
587 flames A, B, and C, respectively. Figure 7 shows that a higher
588 rate $\Omega_T(x,t)$ is statistically linked with a higher normalized
589 dilatation Θ^* , with the highest local values of $\Omega_T(x,t)$ being
590 accompanied by the highest local values of Θ^* , as for $c = 0.75$
591 and 0.90 . The effect is strongly pronounced in case C, where
592 Θ^* can be as large as 12. Note that an increase in Θ^*

FIG. 7. Probability density functions $P(\Theta^*)$ of the normalized dil-
atation conditioned to various ratios of $\Omega_T(x,t)/\max\{\Omega_T(x,t)\}$,
specified in legends. The PDFs have been sampled from the entire
computational domains. (a) Bangalore flame IIS, (b) KAUST flame
A, (c) KAUST flame B, (d) KAUST flame C.

FIG. 8. (a) Probability density functions $P(\delta_L^{-1}\nabla \cdot \mathbf{n})$ of the nor-
malized curvature extracted from different zones of the C flame
brush, characterized by the mean values of the combustion progress
variable specified in legends. (b) Variations in the probabilities of
 $\delta_L^{-1}\nabla \cdot \mathbf{n} > 1$ and $\delta_L^{-1}\nabla \cdot \mathbf{n} < -1$ in the flame brush.

FIG. 9. Extreme (over transverse plane and time) values of (a)
local heat release rate normalized using the peak heat release rate in
the unperturbed laminar flame and (b) normalized dilatation Θ^* vs.
mean combustion progress variable. In the right panel, both positive
and negative extreme values are plotted using the same line style for
each flame, but different colors (red and black, respectively).

unity to 12 (Fig. 7d) yields an increase in the local dilatational
dissipation rate by two orders of magnitude.

Such local perturbations are expected at low values of \bar{c} ,
because positively curved reaction zones are localized at the
leading edge of the mean flame brush. Indeed, Fig. 8a shows
that the PDF of local curvature $\nabla \cdot \mathbf{n}$ normalized using the
laminar flame thickness δ_L is shifted to positive values at the
leading edge ($\bar{c} = 0.05$) when compared to the middle of the
flame brush ($\bar{c} = 0.5$) or its trailing edge ($\bar{c} = 0.95$). As a
result, the probability of $\delta_L^{-1}\nabla \cdot \mathbf{n}$ being larger than unity is
the highest at low \bar{c} and decreases with increasing \bar{c} (Fig. 8b).
On the contrary, the probability of $\delta_L^{-1}\nabla \cdot \mathbf{n} < -1$ is increased
by \bar{c} .

While results reported in Figs. 7 and 8 appear to be consis-
tent with the assumption that the diffusive-thermal effects con-
tribute substantially to significant values of dilatational dissipa-
tion rate observed in Fig. 1f at small \bar{c} , inspection of other
DNS data does not support this hypothesis. For instance, Fig.
9 shows that the maximum (over transverse plane and time)
values of heat release rate and dilatation (i) depend weakly on
the mean combustion progress variable in flames A and B and
(ii) peak at values of \bar{c} that are larger than values of \bar{c} associ-
ated with the highest dilatational dissipation rate in flame C.
The decrease in the extreme values of the normalized Ω_T and
 Θ^* with the mean combustion progress variable is attributed
to the rapid turbulence decay in case C, as seen in Fig. 1f.

Moreover, Fig. 10 indicates that the probability of finding
a local heat release rate larger than its maximum value in the
unperturbed laminar flame peaks in the middle of the flame
brush, rather than at low \bar{c} . Furthermore, Fig. 11 shows that a
ratio of dilatational and solenoidal dissipation rates (the same
rates are plotted in Fig. 1f in another format) does not exhibit
a peak at the leading edge of the flame brush in case C, but is
increased with \bar{c} up to $\bar{c} \approx 0.8$. This increase can be attributed
to the turbulence decay, because the dilatational dissipation
rate plays a more important role at lower Ka , as shown in Fig.
1f.

Thus, results reported in Figs. 10 and 11 imply that the sig-

FIG. 10. Probability of finding a local heat release rate larger than
its maximum value in the unperturbed laminar flame vs. mean combu-
stion progress variable.

This is the author's peer reviewed, accepted manuscript. However, the online version of record will be different from this version once it has been copyedited and typeset.

PLEASE CITE THIS ARTICLE AS DOI: 10.1063/1.50039101

FIG. 11. Ratio of dilatational and solenoidal dissipation rates vs. mean combustion progress variable in flame C.

631 nificant dilatational dissipation rates encountered at low \bar{c} in
632 case C are unlikely to be caused by the diffusive-thermal ef-
633 fects. Indeed, since the mean thickness of flame C is compa-
634 rable with the laminar flame thickness ($\delta_L \approx 3\delta_L$), the proba-
635 bility that reaction zones perturbed by turbulent eddies appear
636 at a low \bar{c} is very low. On the contrary, turbulence-controlled
637 dilatation can be observed in preheat zones at a low \bar{c} and a
638 curve plotted in black dotted lines in Fig. 9b does show that
639 the magnitude of negative (turbulence-controlled) dilatation is
640 highest at low \bar{c} in case C. Accordingly, the significant dilata-
641 tional dissipation rates found at low \bar{c} in case C are associated
642 with the influence of turbulence on molecular mixing in the
643 preheat zones, rather than with the diffusive-thermal ef-
644 fects. Nevertheless, such effects could play a role in the mid-
645 of the flame brush, where (i) the maximum values of the
646 local heat release rate and dilatation are still high (Fig. 9)
647 and (ii) the probability of finding Ω_T larger than its maximum
648 value in the unperturbed laminar flame peaks (Fig. 10). This
649 issue requires further study and will be a subject for future
650 research.

651 IV. CONCLUSIONS

652 DNS data obtained by three independent research groups
653 using different numerical codes and methods (e.g., single-step
654 chemistry and complex chemistry flames) from six different
655 premixed turbulent flames associated with flamelet, thin re-
656 action zone, and broken reaction zone regimes of turbulent
657 burning were analyzed to evaluate total, solenoidal, and di-
658 latational dissipations. Results show that dilatational dissipa-
659 tion can be larger than solenoidal dissipation in the flamelet
660 regime and is also significant even in the thin reaction zone
661 regime.

662 Moreover, certain physical arguments and numerical results
663 imply that dilatational dissipation could play a role even in
664 highly turbulent flames due to the influence of turbulence on
665 molecular mixing in the local flame zones characterized by
666 negligible heat release rate. In particular, due to this phys-
667 ical mechanism, local dilation can be negative and have
668 large magnitude in the leading zone of the highly turbulent
669 flame C ($Ka > 100$). As a result, a ratio of dilatational and
670 solenoidal dissipations does not vanish in that zone, but stays
671 close to 0.15. Moreover, while local dilatation and heat re-
672 lease rate correlate very well in the complex-chemistry flames
673 IIS, A, and B associated with the flamelet and thin reaction
674 zone regimes of premixed turbulent burning, such a correla-
675 tion is substantially less pronounced at low \bar{c} in the complex-
676 chemistry flame C characterized by the highest Karlovitz
677 number, thus, indicating again importance of the turbulence-
678 controlled dilatation in that highly turbulent flame.

679 DNS data obtained from four lean hydrogen-air flames also
680 show that local heat release rate and dilatation can reach val-
681 ues that are significantly (by an order of magnitude in case C)

682 C) larger than the peak values of these quantities in the un-
683 perturbed laminar flames, with the effect magnitudes being
684 increased by Karlovitz number. These findings are attributed
685 to local heating and enrichment of reacting mixture due to im-
686 balance of molecular fluxes of reactants and heat to and from,
687 respectively, reaction zones wrinkled and strained by turbu-
688 lent eddies. Such effects can also contribute to a substantial
689 role played by dilatational dissipation in premixed turbulent
690 flames.

To our knowledge, the present study provides the first evi-
691 dence of the importance of dilatational dissipation in pre-
692 mixed turbulent flames characterized by low Mach numbers.
693 In addition, the study shows that the influence of combustion-
694 induced thermal expansion on dissipation rate is not limited to
695 an increase in the mixture viscosity by the temperature.

A substantial role played by dilatational dissipation in pre-
696 mixed turbulent flames casts doubts on the direct application
697 of conventional constant-density turbulence models for simu-
698 lations of premixed burning. To further investigate dilata-
699 tion and dilatational dissipation in premixed turbulent flames,
700 a parametric DNS study aimed at exploring the function f on
701 the right hand side of Eq. (5) appears to be of interest. To
702 extend the range of considered parameters, such a study could
703 be performed in the case of a single-step chemistry. Moreover,
704 term-by-term analysis of the exact equation for dilatation ap-
705 pears to be of interest also and will be the subject of future
706 work.

ACKNOWLEDGMENTS

The authors are grateful to Prof. Chaudhuri for his valu-
707 able contribution to the DNS of flame IIS. VAS gratefully ac-
708 knowledges the financial support by the Grant of the Ministry
709 of Education and Science of the Russian Federation (Contract
710 No. 14.G39.31.0001 of February 13, 2017). ANL gratefully
711 acknowledges the financial support by the Combustion En-
712 gine Research Center (CERC). HLD acknowledges the com-
713 putational resources provided by the Supercomputer Educa-
714 tion and Research Centre (SERC), IISc for performing the
715 DNS calculation (flame IIS). WS, FEHP, and HGI were spon-
716 sored by King Abdullah University of Science and Technol-
717 ogy (KAUST). Computational resources for the DNSs of
718 flames A, B, and C were provided by the KAUST Supercom-
719 puting Laboratory.

Data availability statement

The data that support the findings of this study are available
720 from the corresponding author upon reasonable request.

¹A. N. Kolmogorov, "The local structure of turbulence in incompressible
721 viscous fluid for very large Reynolds number," *Dokl. Akad. Nauk SSSR*
722 **30**, 299 (1941).

²A. S. Monin and A. M. Yaglom, *Statistical Fluid Mechanics: Mechanics of
723 Turbulence*, vol. 2 (The MIT Press, Cambridge, Massachusetts, 1975).

³L. D. Landau and E. M. Lifshitz, *Fluid Mechanics* (Pergamon Press, Ox-
724 ford, UK, 1987).

⁴U. Frisch, *Turbulence: The Legacy of A.N. Kolmogorov* (Cambridge Uni-
725 versity Press, Cambridge, UK, 1995).

This is the author's peer reviewed, accepted manuscript. However, the online version of record will be different from this version once it has been copyedited and typeset.

PLEASE CITE THIS ARTICLE AS DOI: 10.1063/1.50039101

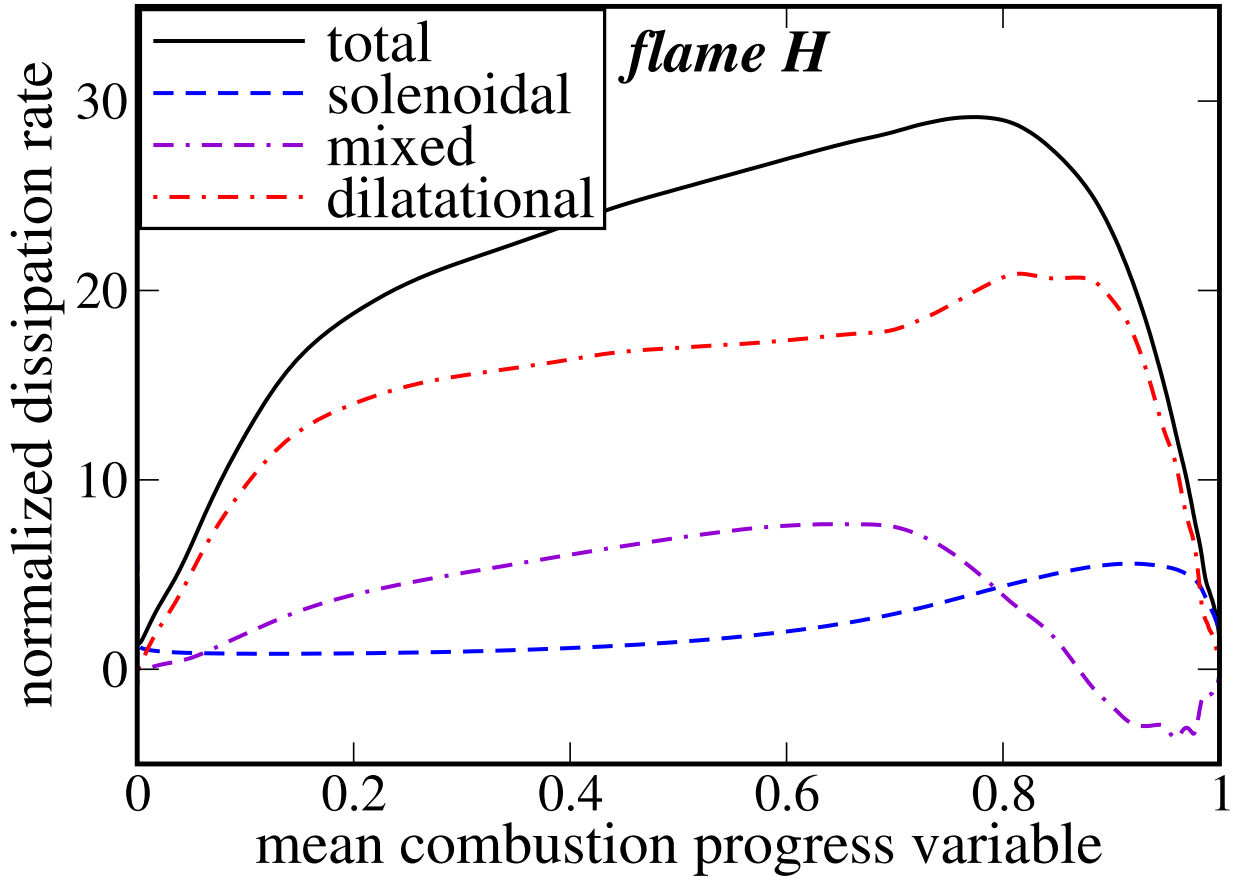
- 736 ⁵S. B. Pope, *Turbulent Flows* (Cambridge University Press, Cambridge, UK, 2000). 807
- 737
- 738 ⁶A. Tsinober, *An Informal Conceptual Introduction to Turbulence* (Springer, Heidelberg, Germany, 2009). 809
- 739
- 740 ⁷S. K. Lele, "Compressibility effects on turbulence," *Annu. Rev. Fluid Mech.* **26**, 211 (1994). 811
- 741
- 742 ⁸P. G. Huang, G. N. Coleman, and P. Bradshaw, "Compressible turbulence in channel flows: DNS results and modeling," *J. Fluid Mech.* **305**, 185 (1995). 813
- 743
- 744 ⁹V. M. Canuto, "Compressible turbulence," *Astr. J.* **482**, 827 (1997). 814
- 745
- 746 ¹⁰R. Friedrich and F. P. Bertolotti, "Compressibility effects due to turbulence fluctuations," *Appl. Sci. Res.* **57**, 165 (1997). 816
- 747
- 748 ¹¹Y. Andreopoulos, J. H. Agui, and G. Briassulis, "Shock wave-turbulence interactions," *Annu. Rev. Fluid Mech.* **32**, 309 (2000). 818
- 749
- 750 ¹²O. Zeman, "Dilatation dissipation: the concept and application in modeling compressible mixing layers," *Phys. Fluids A* **2**, 78 (1990). 820
- 751
- 752 ¹³S. Jagannathan and D. A. Donzis, "Reynolds and Mach number scaling in solenoidally-forced compressible turbulence using high-resolution direct numerical simulations," *J. Fluid Mech.* **789**, 669 (2016). 823
- 753
- 754 ¹⁴J. Wang, T. Gotoh, and T. Watanabe, "Spectra and statistics in compressible isotropic turbulence," *Phys. Rev. Fluids* **2**, 013403 (2017). 825
- 755
- 756 ¹⁵J. P. John, D. A. Donzis, and K. R. Sreenivasan, "Solenoidal scaling laws for compressible mixing," *Phys. Rev. Lett.* **123**, 224501 (2019). 827
- 757
- 758 ¹⁶J. Teng, J. Wang, H. Li, and S. Chen, "Spectra and scaling in chemically reacting compressible isotropic turbulence," *Phys. Rev. Fluids* **5**, 084602 (2020). 830
- 759
- 760 ¹⁷D. A. Donzis and J. P. John, "Universality and scaling in homogeneous compressible turbulence," *Phys. Rev. Fluids* **5**, 084609 (2020). 832
- 761
- 762 ¹⁸J. P. John, D. A. Donzis, and K. R. Sreenivasan, "Compressibility effects on the scalar dissipation rate," *Combust. Sci. Technol.* **192**, 1320 (2020). 834
- 763
- 764 ¹⁹F. A. Jaber and C. K. Madnia, "Effects of heat of reaction on homogeneous compressible turbulence," *J. Sci. Computing* **13**, 201 (1998). 836
- 765
- 766 ²⁰M. P. Martin and G. Candler, "Effect of chemical reactions on decaying isotropic turbulence," *Phys. Fluids* **10**, 1715 (1998). 837
- 767
- 768 ²¹F. A. Jaber, D. Livescu, and C. K. Madnia, "Characteristics of chemically reacting compressible homogeneous turbulence," *Phys. Fluids* **12**, 1189 (2000). 841
- 769
- 770 ²²D. Livescu, F. A. Jaber, and C. K. Madnia, "The effects of heat release on the energy exchange in reacting turbulent shear flow," *J. Fluid Mech.* **450**, 35 (2002). 844
- 771
- 772 ²³S. D. Mason and C. J. Rutland, "Turbulent transport in spatially developing reacting shear layers," *Proc. Combust. Inst.* **28**, 505 (2000). 846
- 773
- 774 ²⁴B. Bobbitt and G. Blanquart, "Vorticity isotropy in high Karlovitz number premixed flames," *Phys. Fluids* **28**, 105101 (2016). 847
- 775
- 776 ²⁵B. Bobbitt, S. Lapointe, and G. Blanquart, "Vorticity transformation in high Karlovitz number premixed flames," *Phys. Fluids* **28**, 015101 (2016). 850
- 777
- 778 ²⁶A. N. Lipatnikov and J. Chomiak, "Effects of premixed flames on turbulence and turbulent scalar transport," *Prog. Energy Combust. Sci.* **36**, 182 (2010). 853
- 779
- 780 ²⁷V. A. Sabelnikov and A. N. Lipatnikov, "Recent advances in understanding of thermal expansion effects in premixed turbulent flames," *Annu. Rev. Fluid Mech.* **49**, 91 (2017). 856
- 781
- 782 ²⁸S. Nishiki, T. Hasegawa, R. Borghi, and R. Himeno, "Modeling of flame-generated turbulence based on direct numerical simulation databases," *Proc. Combust. Inst.* **29**, 2017 (2002). 859
- 783
- 784 ²⁹S. Nishiki, T. Hasegawa, R. Borghi, and R. Himeno, "Modelling of turbulent scalar flux in turbulent premixed flames based on DNS databases," *Combust. Theory Modelling* **10**, 39 (2006). 862
- 785
- 786 ³⁰Y. H. Im, K. Y. Huh, S. Nishiki, and T. Hasegawa, "Zone conditional assessment of flame-generated turbulence with DNS database of a turbulent premixed flame," *Combust. Flame* **137**, 478 (2004). 865
- 787
- 788 ³¹A. Mura, K. Tsuboi, and T. Hasegawa, "Modelling of the correlation between velocity and reactive scalar gradients in turbulent premixed flames based on DNS data," *Combust. Theory Modelling* **12**, 671 (2008). 867
- 789
- 790 ³²A. Mura, V. Robin, M. Champion, and T. Hasegawa, "Small scale features of velocity and scalar fields in turbulent premixed flames," *Flow Turbulence Combust.* **82**, 339 (2009). 871
- 791
- 792 ³³V. Robin, A. Mura, M. Champion, and T. Hasegawa, "Direct and indirect thermal expansion effects in turbulent premixed flames," *Combust. Sci. Technol.* **182**, 449 (2010). 874
- 793
- 794 ³⁴V. Robin, A. Mura, and M. Champion, "Modeling of the effects of thermal expansion on scalar turbulent fluxes in turbulent premixed flames," *J. Fluid Mech.* **689**, 149 (2011).
- 795
- 796 ³⁵K. N. C. Bray, M. Champion, P. A. Libby, and N. Swaminathan, "Scalar dissipation and mean reaction rates in premixed turbulent combustion," *Combust. Flame* **158**, 2017 (2011).
- 797
- 798 ³⁶A. N. Lipatnikov, S. Nishiki, and T. Hasegawa, "A direct numerical simulation study of vorticity transformation in weakly turbulent premixed flames," *Phys. Fluids* **26**, 105104 (2014).
- 799
- 800 ³⁷A. N. Lipatnikov, S. Nishiki, and T. Hasegawa, "DNS assessment of relation between mean reaction and scalar dissipation rates in the flamelet regime of premixed turbulent combustion," *Combust. Theory Modell.* **19**, 309 (2015).
- 801
- 802 ³⁸A. N. Lipatnikov, J. Chomiak, V. A. Sabelnikov, S. Nishiki, and T. Hasegawa, "Unburned mixture fingers in premixed turbulent flames," *Proc. Combust. Inst.* **35**, 1401 (2015).
- 803
- 804 ³⁹A. N. Lipatnikov, V. A. Sabelnikov, S. Nishiki, T. Hasegawa, and N. Chakraborty, "DNS assessment of a simple model for evaluating velocity conditioned to unburned gas in premixed turbulent flames," *Flow Turbul. Combust.* **94**, 513 (2015).
- 805
- 806 ⁴⁰V. A. Sabelnikov, A. N. Lipatnikov, N. Chakraborty, S. Nishiki, and T. Hasegawa, "A transport equation for reaction rate in turbulent flows," *Phys. Fluids* **28**, 081701 (2016).
- 807
- 808 ⁴¹V. A. Sabelnikov, A. N. Lipatnikov, N. Chakraborty, S. Nishiki, and T. Hasegawa, "A balance mixture fingers for the mean rate of product creation in premixed turbulent flames," *Proc. Combust. Inst.* **36**, 1893 (2017).
- 809
- 810 ⁴²A. N. Lipatnikov, V. A. Sabelnikov, S. Nishiki, and T. Hasegawa, "Flamelet perturbations and flame surface density transport in weakly turbulent premixed combustion," *Combust. Theory Modell.* **21**, 205 (2017).
- 811
- 812 ⁴³A. N. Lipatnikov, J. Chomiak, V. A. Sabelnikov, S. Nishiki, and T. Hasegawa, "A DNS study of the physical mechanisms associated with density ratio influence on turbulent burning velocity in premixed flames," *Combust. Theory Modell.* **22**, 131 (2018).
- 813
- 814 ⁴⁴A. N. Lipatnikov, V. A. Sabelnikov, N. Chakraborty, S. Nishiki, and T. Hasegawa, "A DNS study of closure relations for convection flux term in transport equation for mean reaction rate in turbulent flow," *Flow Turbul. Combust.* **100**, 75 (2018).
- 815
- 816 ⁴⁵A. N. Lipatnikov, V. A. Sabelnikov, S. Nishiki, and T. Hasegawa, "Combustion-induced local shear layers within premixed flamelets in weakly turbulent flows," *Phys. Fluids* **30**, 085101 (2018).
- 817
- 818 ⁴⁶A. N. Lipatnikov, V. A. Sabelnikov, S. Nishiki, and T. Hasegawa, "Does flame-generated vorticity increase turbulent burning velocity?" *Phys. Fluids* **30**, 081702 (2018).
- 819
- 820 ⁴⁷A. N. Lipatnikov, S. Nishiki, and T. Hasegawa, "A DNS assessment of linear relations between filtered reaction rate, flame surface density, and scalar dissipation rate in a weakly turbulent premixed flame," *Combust. Theory Modell.* **23**, 245 (2019).
- 821
- 822 ⁴⁸A. N. Lipatnikov, S. Nishiki, and T. Hasegawa, "Closure relations for fluxes of flame surface density and scalar dissipation rate in turbulent premixed flames," *Fluids* **4**, 43 (2019).
- 823
- 824 ⁴⁹A. N. Lipatnikov, V. A. Sabelnikov, S. Nishiki, and T. Hasegawa, "A direct numerical simulation study of the influence of flame-generated vorticity on reaction-zone-surface area in weakly turbulent premixed combustion," *Phys. Fluids* **31**, 055101 (2019).
- 825
- 826 ⁵⁰V. A. Sabelnikov, A. N. Lipatnikov, S. Nishiki, and T. Hasegawa, "Application of conditioned structure functions to exploring influence of premixed combustion on two-point turbulence statistics," *Proc. Combust. Inst.* **37**, 2433 (2019).
- 827
- 828 ⁵¹V. A. Sabelnikov, A. N. Lipatnikov, S. Nishiki, and T. Hasegawa, "Investigation of the influence of combustion-induced thermal expansion on two-point turbulence statistics using conditioned structure functions," *J. Fluid Mech.* **867**, 45 (2019).
- 829
- 830 ⁵²V. A. Sabelnikov, A. N. Lipatnikov, N. Nikitin, S. Nishiki, and T. Hasegawa, "Application of Helmholtz-Hodge decomposition and conditioned structure functions to exploring influence of premixed combustion on turbulence upstream of the flame," *Proc. Combust. Inst.* **38**, <https://doi.org/10.1016/j.proci.2020.09.015>.
- 831
- 832 ⁵³V. A. Sabelnikov, A. N. Lipatnikov, N. Nikitin, S. Nishiki, and T. Hasegawa, "Solenoidal and potential velocity fields in weakly turbulent premixed flames," *Proc. Combust. Inst.* **38**, <https://doi.org/10.1016/j.proci.2020.09.016>.

This is the author's peer reviewed, accepted manuscript. However, the online version of record will be different from this version once it has been copyedited and typeset.

PLEASE CITE THIS ARTICLE AS DOI: 10.1063/5.0039101

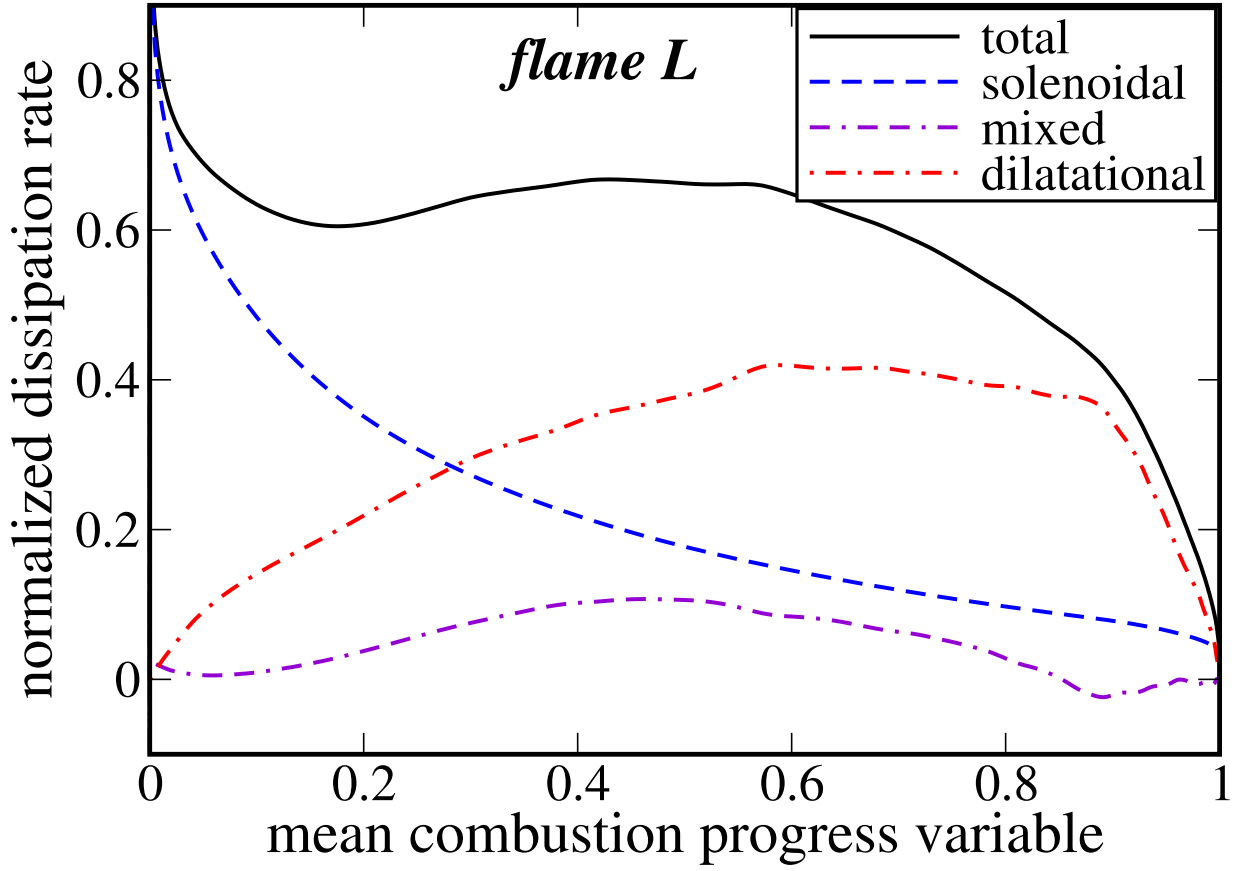
- 876 ⁵⁴A. N. Lipatnikov, V. A. Sabelnikov, S. Nishiki, and T. Hasegawa, "Influence
877 of thermal expansion on potential and rotational components of turbulent
878 velocity field within and upstream of premixed flame brush," *Flow Turbul.*
879 *Combust.* <https://doi.org/10.1007/s10494-020-00131-3>. 933
- 880 ⁵⁵H. Dave and S. Chaudhuri, "Evolution of local flame displacement speed
881 in turbulence," *J. Fluid Mech.* **884**, A46 (2020). 935
- 882 ⁵⁶A. N. Lipatnikov and V. A. Sabelnikov, "An extended flamelet-based pre-
883 sumed probability density function for predicting mean concentrations of
884 various species in premixed turbulent flames," *Int. J. Hydrogen Energy* **45**,
885 31162 (2020). 939
- 886 ⁵⁷A. N. Lipatnikov and V. A. Sabelnikov, "Evaluation of mean species mass
887 fractions in premixed turbulent flames: A DNS study," *Proc. Combust. Inst.*
888 **38**, <https://doi.org/10.1016/j.proci.2020.05.006>. 942
- 889 ⁵⁸H. G. Im, P. G. Arias, S. Chaudhuri, and H. A. Urañakara, "Direct numerical
890 simulations of statistically stationary turbulent premixed flames," *Combust.*
891 *Sci. Technol.* **188**, 1182 (2016). 945
- 892 ⁵⁹H. A. Urañakara, S. Chaudhuri, H. L. Dave, P. G. Arias, and H. G. Im,
893 "A flame particle tracking analysis of turbulence-chemistry interaction in
894 hydrogen-air premixed flames," *Combust. Flame* **163**, 220 (2016). 948
- 895 ⁶⁰D. H. Wacks, N. Chakraborty, M. Klein, P. G. Arias, and H. G. Im, "Flow
896 topologies in different regimes of premixed turbulent combustion: A direct
897 numerical simulation analysis," *Phys. Rev. Fluids* **1**, 083401 (2016). 951
- 898 ⁶¹M. Klein, A. Herbert, H. Kosaka, B. Böhm, A. Dreizler, N. Chakraborty,
899 V. Papadopolou, H. G. Im, and J. Hasslberger, "Evaluation of flame
900 area based on detailed chemistry DNS of premixed turbulent hydrogen-air
901 flames in different regimes of combustion," *Flow Turbul. Combust.* **104**,
902 403 (2020). 956
- 903 ⁶²D. M. Manias, E. A. Tingas, F. E. Hernández-Pérez, R. M. Galassi,
904 P. P. Ciottoli, M. Valorani, and H. G. Im, "Investigation of the turbulent
905 flame structure and topology at different Karlovitz numbers using the tan-
906 gential stretching rate index," *Combust. Flame* **200**, 155 (2019). 960
- 907 ⁶³A. N. Lipatnikov, V. A. Sabelnikov, F. E. Hernández-Pérez, W. Song, and
908 H. G. Im, "A priori DNS study of applicability of flamelet concept to pre-
909 dicting mean concentrations of species in turbulent premixed flames at var-
910 ious Karlovitz numbers," *Combust. Flame* **222**, 370 (2020). 964
- 911 ⁶⁴A. N. Lipatnikov, V. A. Sabelnikov, F. E. Hernández-Pérez, W. Song, and
912 H. G. Im, "Prediction of mean radical concentrations in lean hydrogen-air
913 turbulent flames at different Karlovitz numbers adopting a newly extended
914 flamelet-based presumed PDF," *Combust. Flame* **226**, 248 (2021). 968
- 915 ⁶⁵N. Peters, "The turbulent burning velocity for large-scale and small-scale
916 turbulence," *J. Fluid Mech.* **384**, 107 (1999). 970
- 917 ⁶⁶N. Babkovskaia, N. E. L. Haugen, and A. Brandenburg, "A high-order pub-
918 lic domain code for direct numerical simulations of turbulent combustion,"
919 *J. Comput. Phys.* **230**, 1 (2011). 973
- 920 ⁶⁷J. Li, Z. Zhao, A. Kazakov, and F. L. Dryer, "An updated comprehen-
921 sive kinetic model of hydrogen combustion," *Int. J. Chem. Kinetics* **36**,
922 566 (2004). 976
- 923 ⁶⁸M. P. Burke, M. Chaos, Y. Ju, F. L. Dryer, and S. J. Klippenstein, "Compre-
924 hensive H₂/O₂ kinetic model for high-pressure combustion," *Int. J. Chem.*
925 *Kinet.* **44**, 444 (2012). 978
- 926 ⁶⁹V. R. Kuznetsov and V. A. Sabelnikov, *Turbulence and Combustion* (Hemi-
927 sphere Publ. Corp., New York, 1990). 981
- 928 ⁷⁰A. N. Lipatnikov and J. Chomiak, "Molecular transport effects on turbulent
929 flame propagation and structure," *Prog. Energy Combust. Sci.* **31**, 1 (2005). 984
- ⁷¹A. Lipatnikov, *Fundamentals of Premixed Turbulent Combustion* (CRC
Press, Boca Raton, Florida, 2012).
- ⁷²R. W. Bilger, "Some aspects of scalar dissipation," *Flow Turbul. Combust.*
72, 93 (2004).
- ⁷³J. F. MacArt, T. Grenga, and M. E. Mueller, "Effects of combustion heat
release on velocity and scalar statistics in turbulent premixed jet flames at
low and high Karlovitz numbers," *Combust. Flame* **191**, 468 (2018).
- ⁷⁴J. F. MacArt, T. Grenga, and M. E. Mueller, "Evolution of flame-
conditioned velocity statistics in turbulent premixed jet flames at varying
Karlovitz number," *Proc. Combust. Inst.* **37**, 2503 (2019).
- ⁷⁵V. A. Sabelnikov, R. Yu, and A. N. Lipatnikov, "Thin reaction zones in
constant-density turbulent flows at low Damköhler numbers: Theory and
simulations," *Phys. Fluids* **31**, 055104 (2019).
- ⁷⁶Ya. B. Zel'dovich, G. I. Barenblatt, V. B. Librovich, and G. M. Makhvi-
ladze, *The Mathematical Theory of Combustion and Explosions* (Consul-
tants Burea, New York, 1985).
- ⁷⁷N. Peters, *Turbulent Combustion* (Cambridge University Press, Cambridge,
UK, 2000).
- ⁷⁸T. Poinso and D. Veynante, *Theoretical and Numerical Combustion*, sec-
ond ed. (Edwards, Philadelphia, 2005).
- ⁷⁹A. G. Prudnikov, "Burning of homogeneous fuel-air mixtures in a turbulent
flow," in *Physica Principles of the Working Process in Combustion Cham-
bers of Jet Engines*, edited by B. V. Raushenbakh (Clearing House for Fed-
eral Scientific & Technical Information, Springfield, 1967), pp. 244-336.
- ⁸⁰N. Chakraborty and R. S. Cant, "Influence of Lewis number on curvature
effects in turbulent premixed flame propagation in the thin reaction zone
regime," *Phys. Fluids* **17**, 105105 (2005).
- ⁸¹G. Troiani, F. Battista, and F. Picano, "Turbulent consumption speed via lo-
cal dilatation rate measurements in a premixed bunsen jet," *Combust. Flame*
160, 2029 (2013).
- ⁸²I. Gran, T. Echehki, and J. H. Chen, "Negative flame speed in an un-
steady 2-D premixed flame: a computational study," *Proc. Combust. Inst.*
26, 323 (1996).
- ⁸³N. Peters, P. Terhoeven, J. H. Chen, and T. Echehki, "Statistics of flame dis-
placement speeds from computations of 2-D unsteady methane-air flames,"
Proc. Combust. Inst. **27**, 833 (1998).
- ⁸⁴N. Chakraborty, M. Klein, and R. S. Cant, "Stretch rate effects on displace-
ment speed in turbulent premixed flame kernels in the thin reaction zone
regime," *Proc. Combust. Inst.* **31**, 1385 (2007).
- ⁸⁵H. Wang, E. R. Hawkes, and J. H. Chen, "A direct numerical simula-
tion study of flame structure and stabilization of an experimental high Ka
CH₄/air premixed jet flame," *Combust. Flame* **180**, 110 (2017).
- ⁸⁶S. Luca, A. Attili, E. L. Schiavo, F. Creta, and F. Bisetti, "On the statistics
of flame stretch in turbulent premixed jet flames in the thin reaction zone
regime at varying Reynolds number," *Proc. Combust. Inst.* **37**, 2451 (2019).
- ⁸⁷R. Yu, T. Nilsson, C. Fureby, and A. Lipatnikov, "Evolution equations for
the decomposed components of displacement speed in a reactive scalar
field," *J. Fluid Mech.*, in press.
- ⁸⁸P. Clavin, "Dynamical behavior of premixed flame fronts in laminar and
turbulent flows," *Prog. Energy Combust. Sci.* **11**, 1 (1985).
- ⁸⁹A. M. Klimov, "Laminar flame in a turbulent flow," *Zh. Prikl. Mekh.*
Tekhn. Fiz. **4**, No. 3, 49 (1963).

This is the author's peer reviewed, accepted manuscript. However, the online version of record will be different from this version once it has been copyedited and typeset.
 PLEASE CITE THIS ARTICLE AS DOI: 10.1063/1.50039101



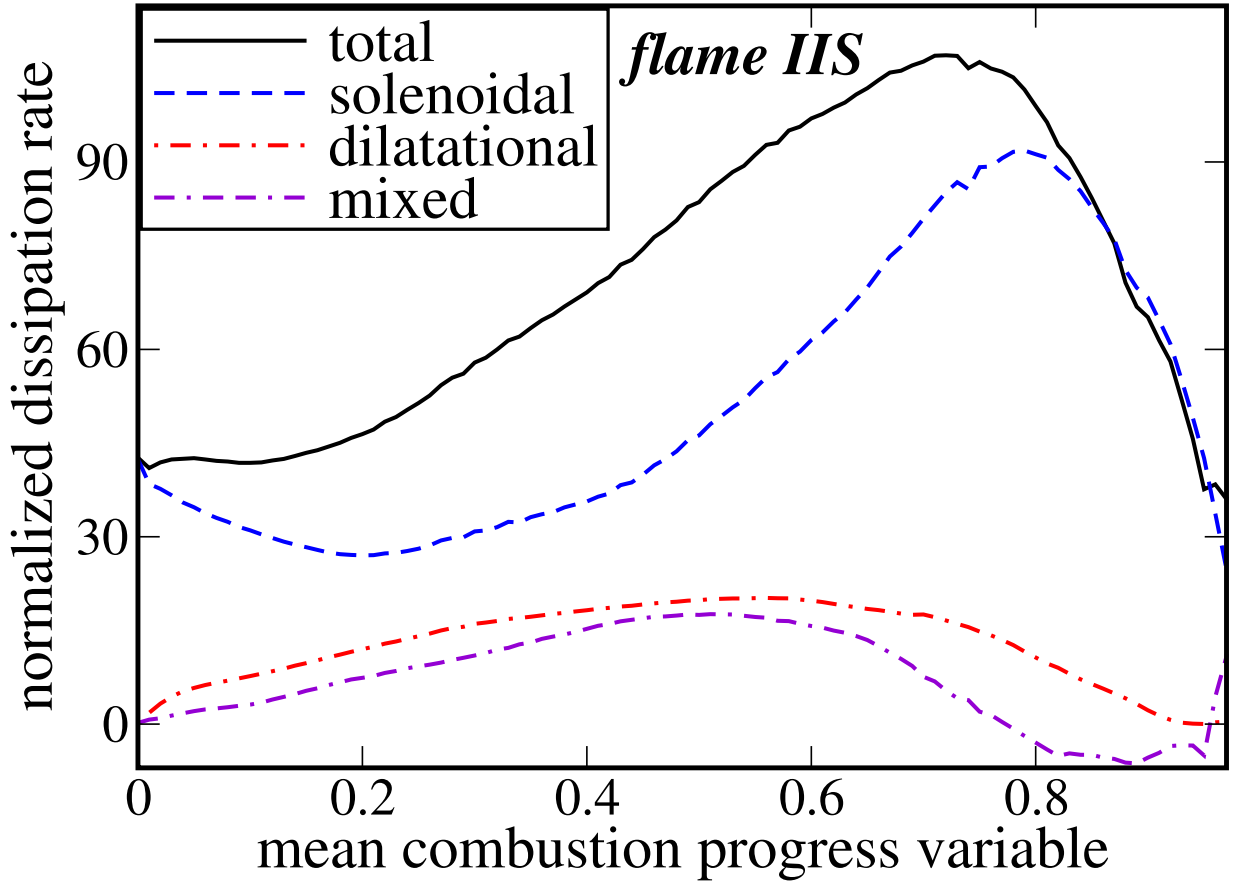
This is the author's peer reviewed, accepted manuscript. However, the online version of record will be different from this version once it has been copyedited and typeset.

PLEASE CITE THIS ARTICLE AS DOI: 10.1063/1.50039101

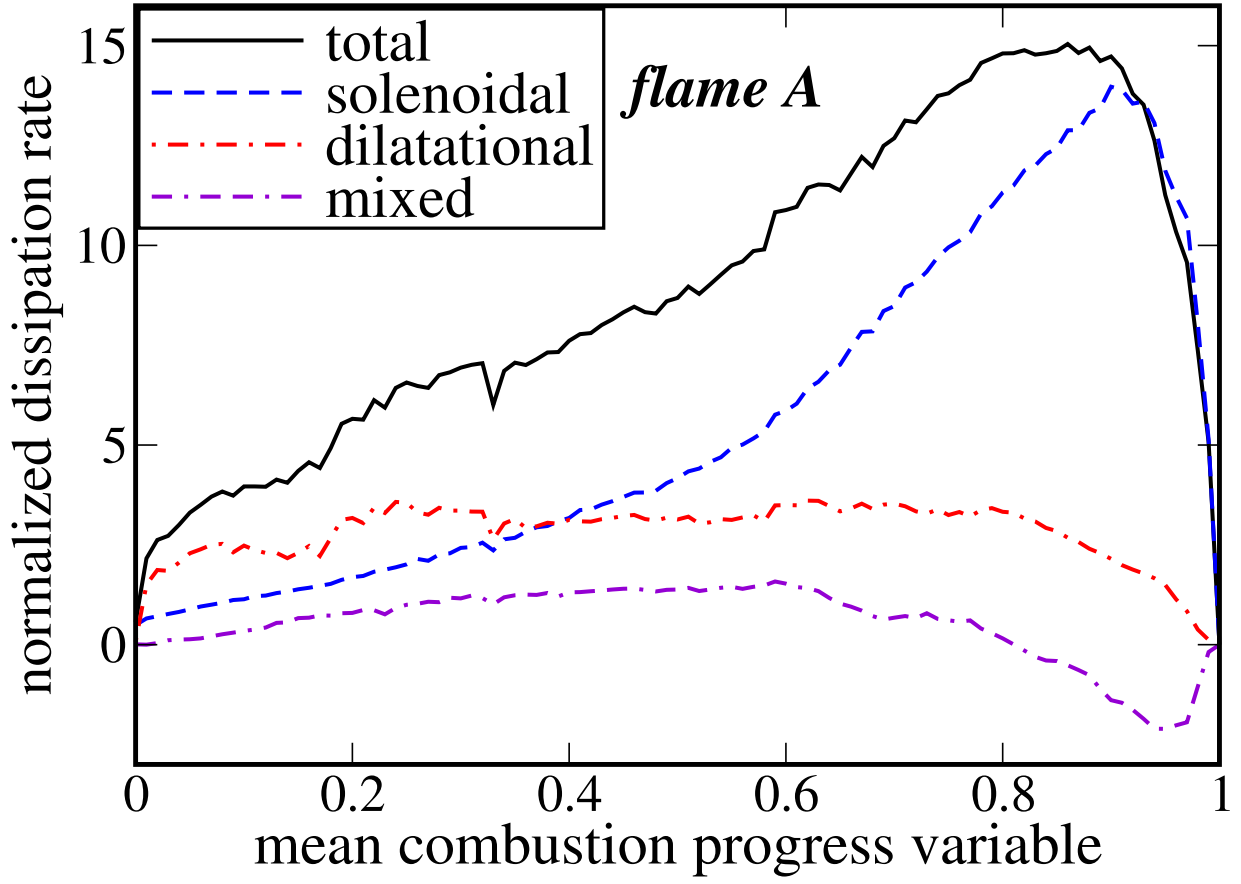


This is the author's peer reviewed, accepted manuscript. However, the online version of record will be different from this version once it has been copyedited and typeset.

PLEASE CITE THIS ARTICLE AS DOI: 10.1063/1.50039101

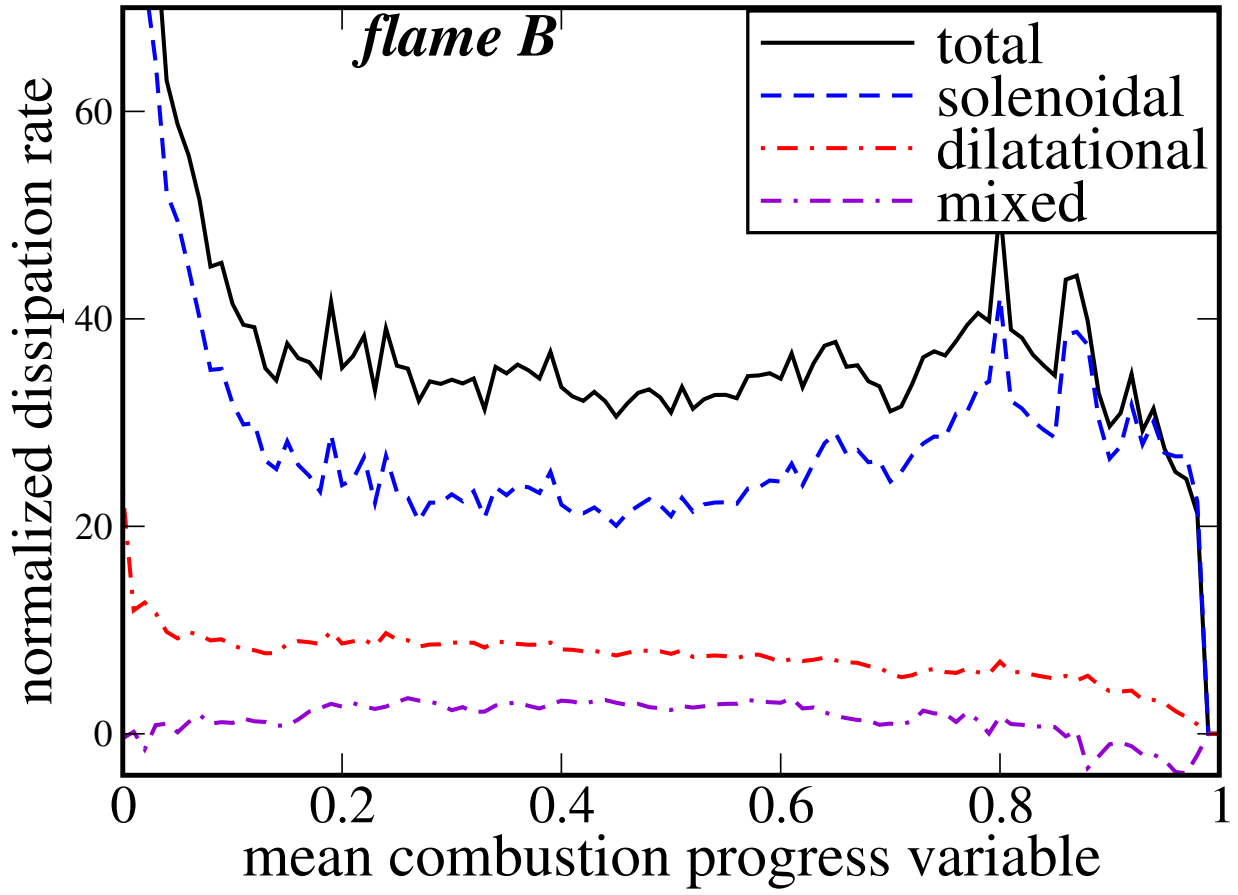


This is the author's peer reviewed, accepted manuscript. However, the online version of record will be different from this version once it has been copyedited and typeset.
PLEASE CITE THIS ARTICLE AS DOI: 10.1063/1.50039101

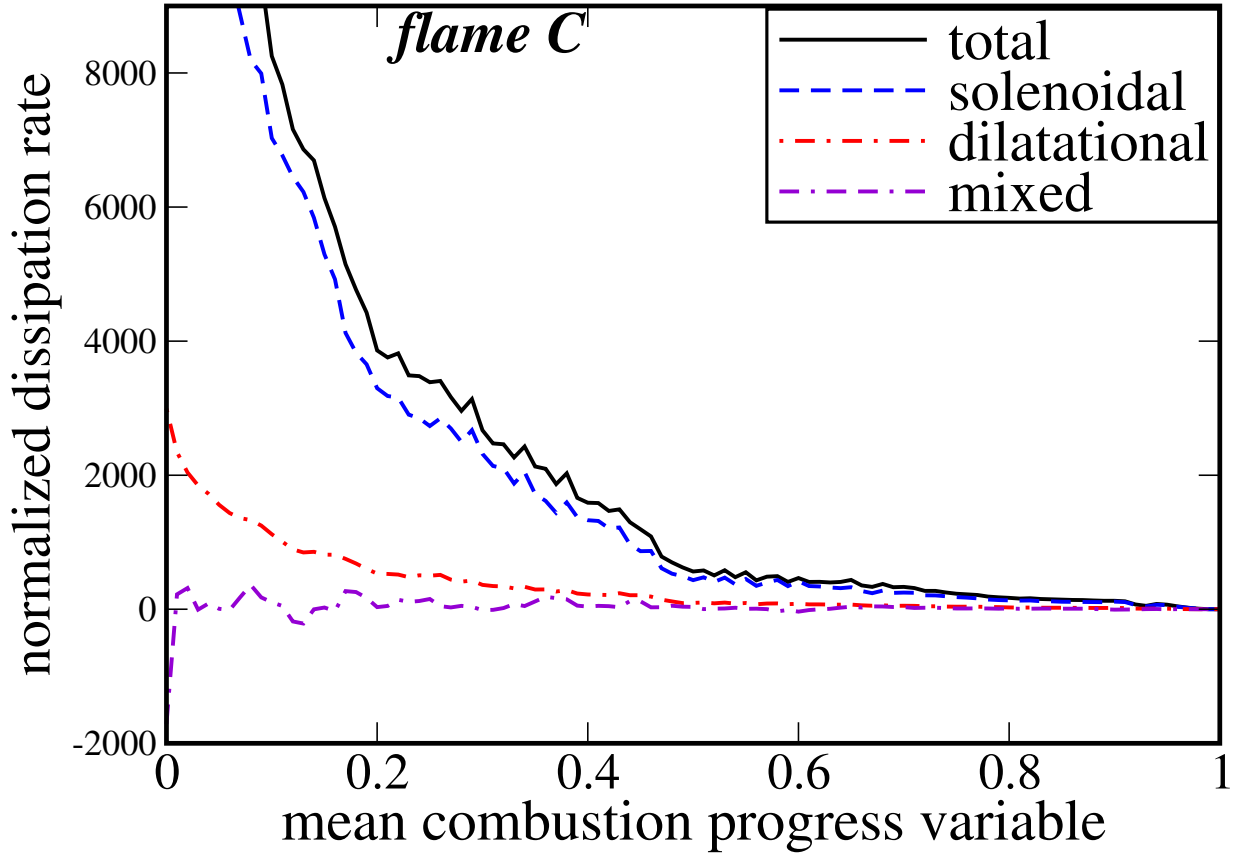


This is the author's peer reviewed, accepted manuscript. However, the online version of record will be different from this version once it has been copyedited and typeset.

PLEASE CITE THIS ARTICLE AS DOI: 10.1063/1.50039101

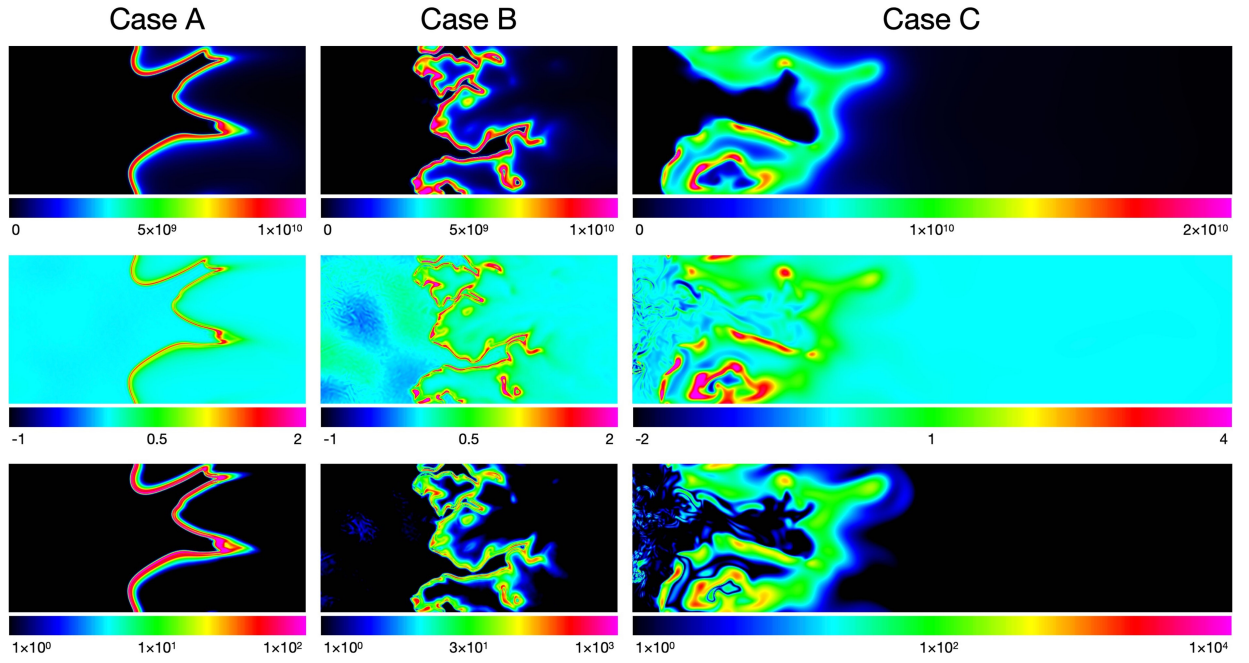


This is the author's peer reviewed, accepted manuscript. However, the online version of record will be different from this version once it has been copyedited and typeset.
 PLEASE CITE THIS ARTICLE AS DOI: 10.1063/1.50039101

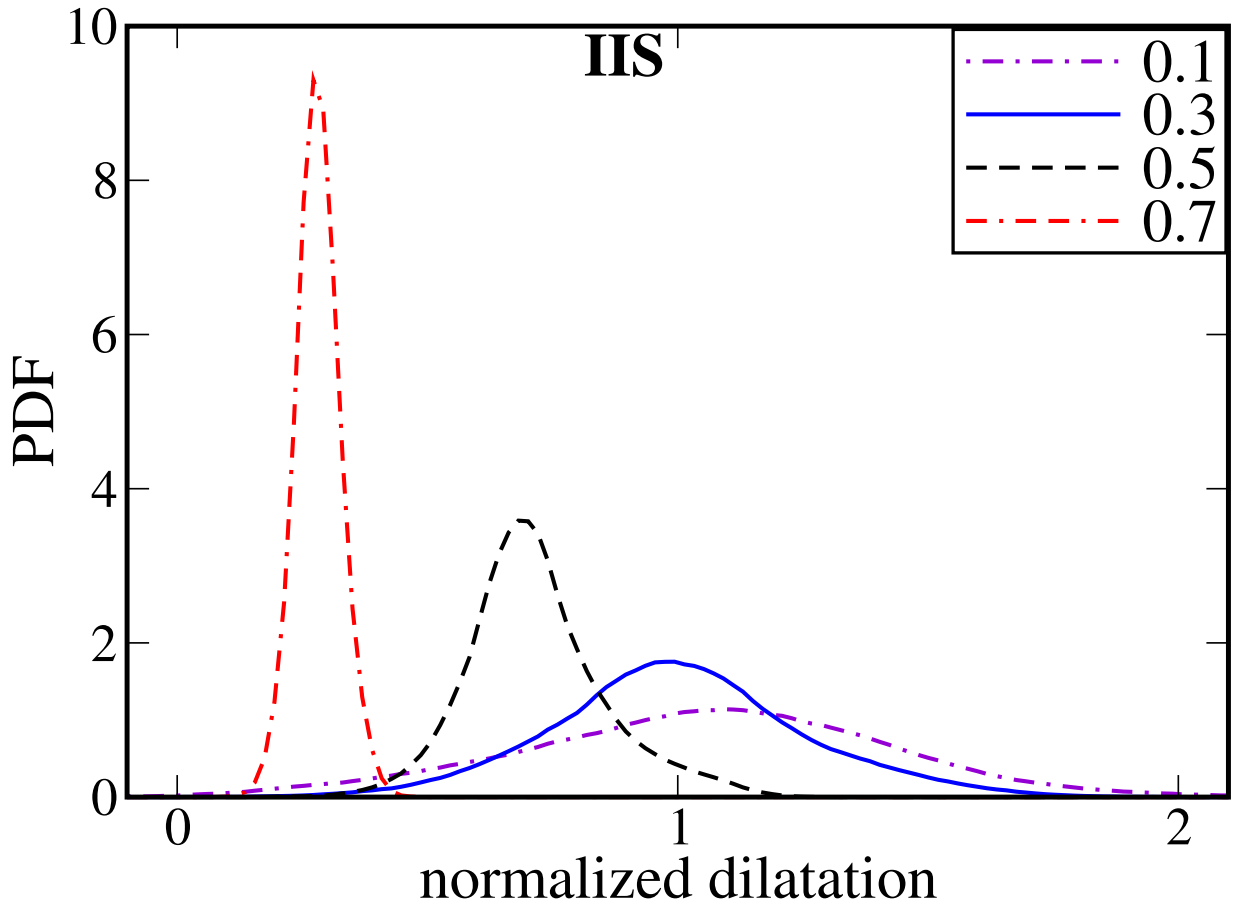


This is the author's peer reviewed, accepted manuscript. However, the online version of record will be different from this version once it has been copyedited and typeset.

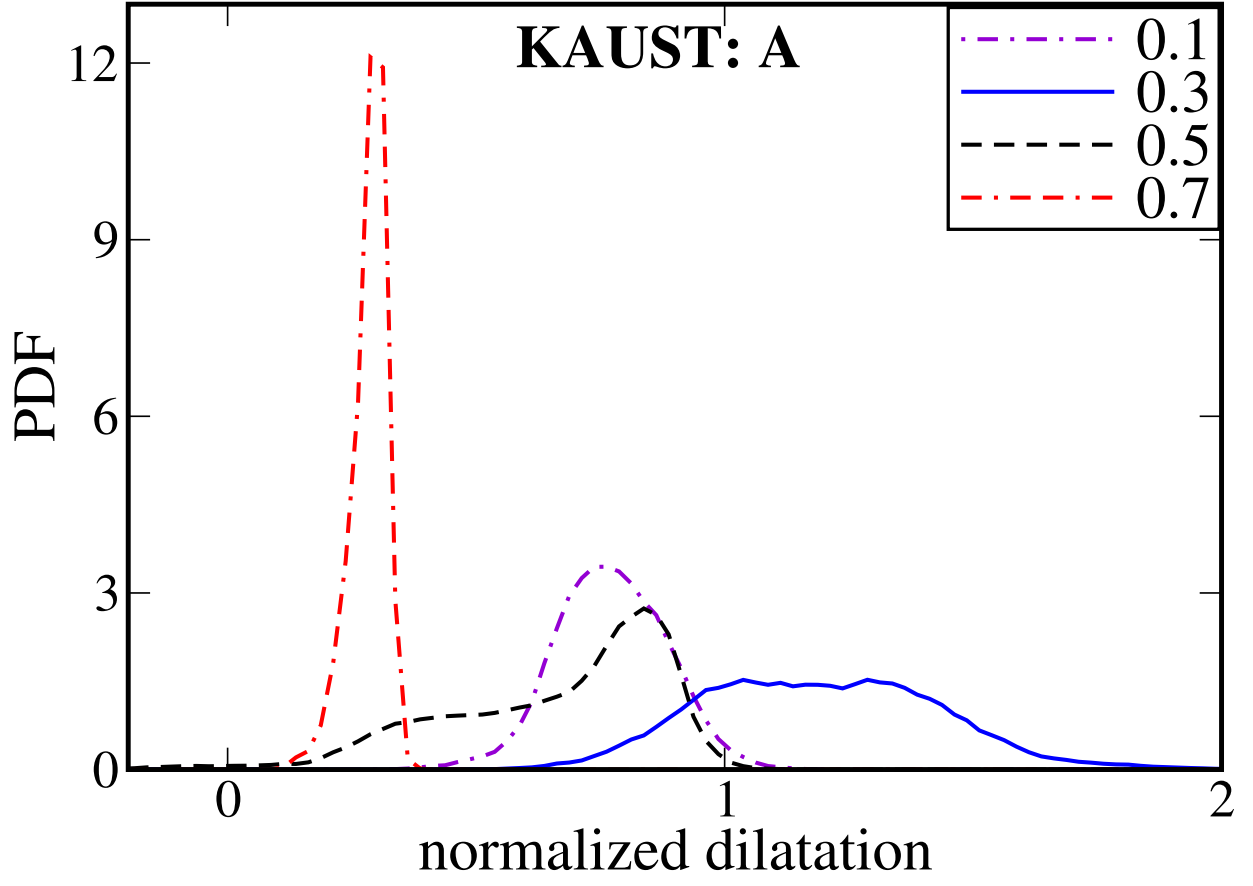
PLEASE CITE THIS ARTICLE AS DOI: 10.1063/1.50039101



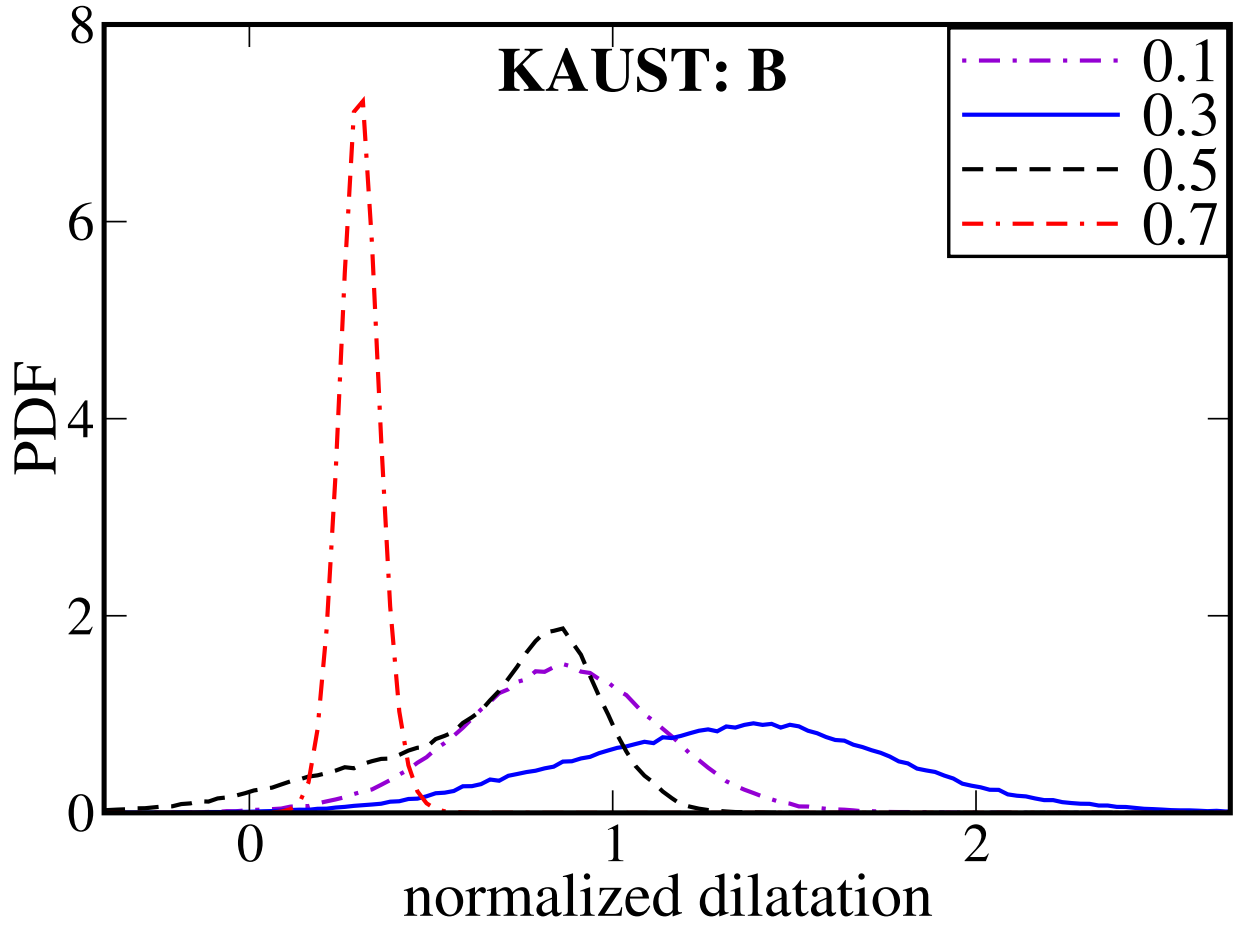
This is the author's peer reviewed, accepted manuscript. However, the online version of record will be different from this version once it has been copyedited and typeset.
PLEASE CITE THIS ARTICLE AS DOI: 10.1063/1.50039101



This is the author's peer reviewed, accepted manuscript. However, the online version of record will be different from this version once it has been copyedited and typeset.
 PLEASE CITE THIS ARTICLE AS DOI: 10.1063/5.0039101

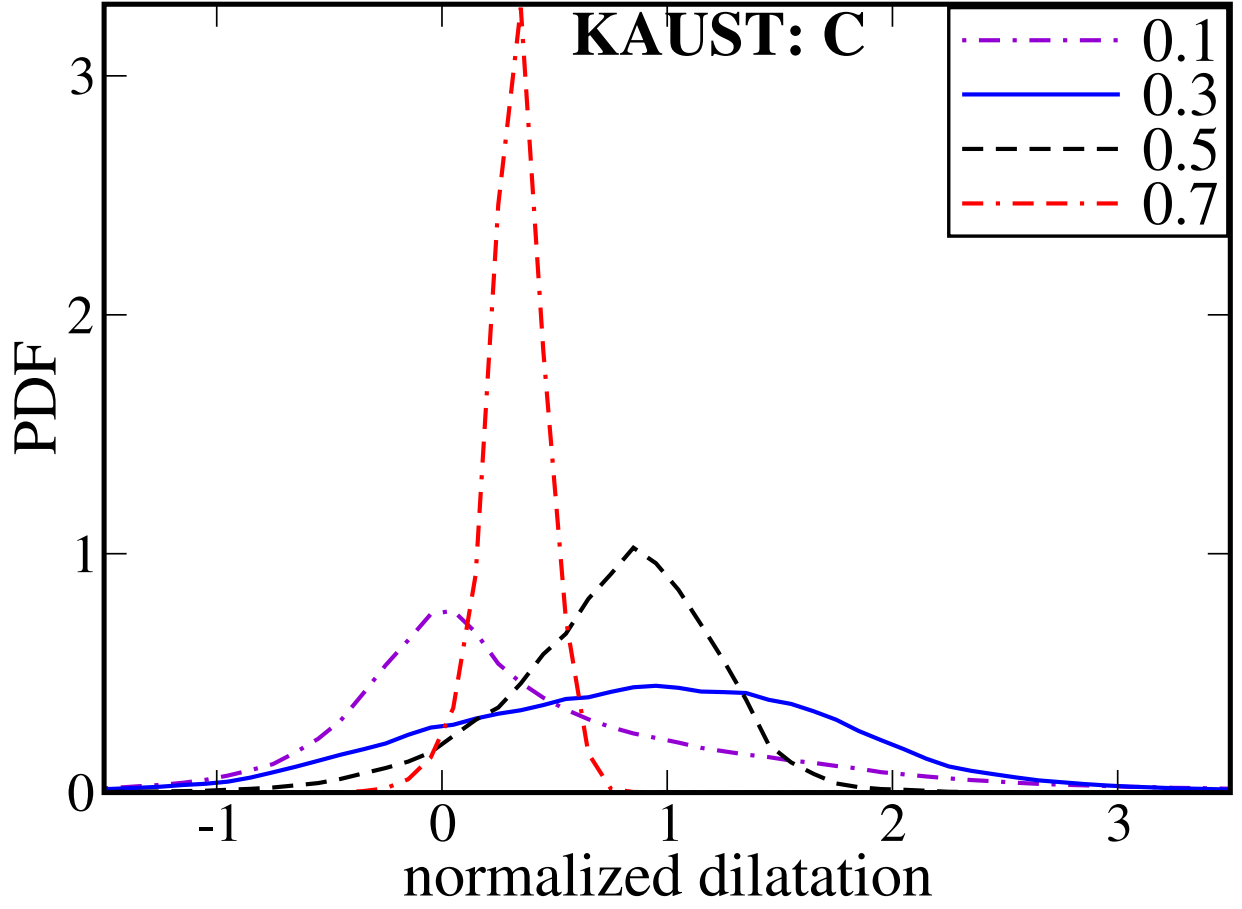


This is the author's peer reviewed, accepted manuscript. However, the online version of record will be different from this version once it has been copyedited and typeset.
PLEASE CITE THIS ARTICLE AS DOI: 10.1063/1.50039101



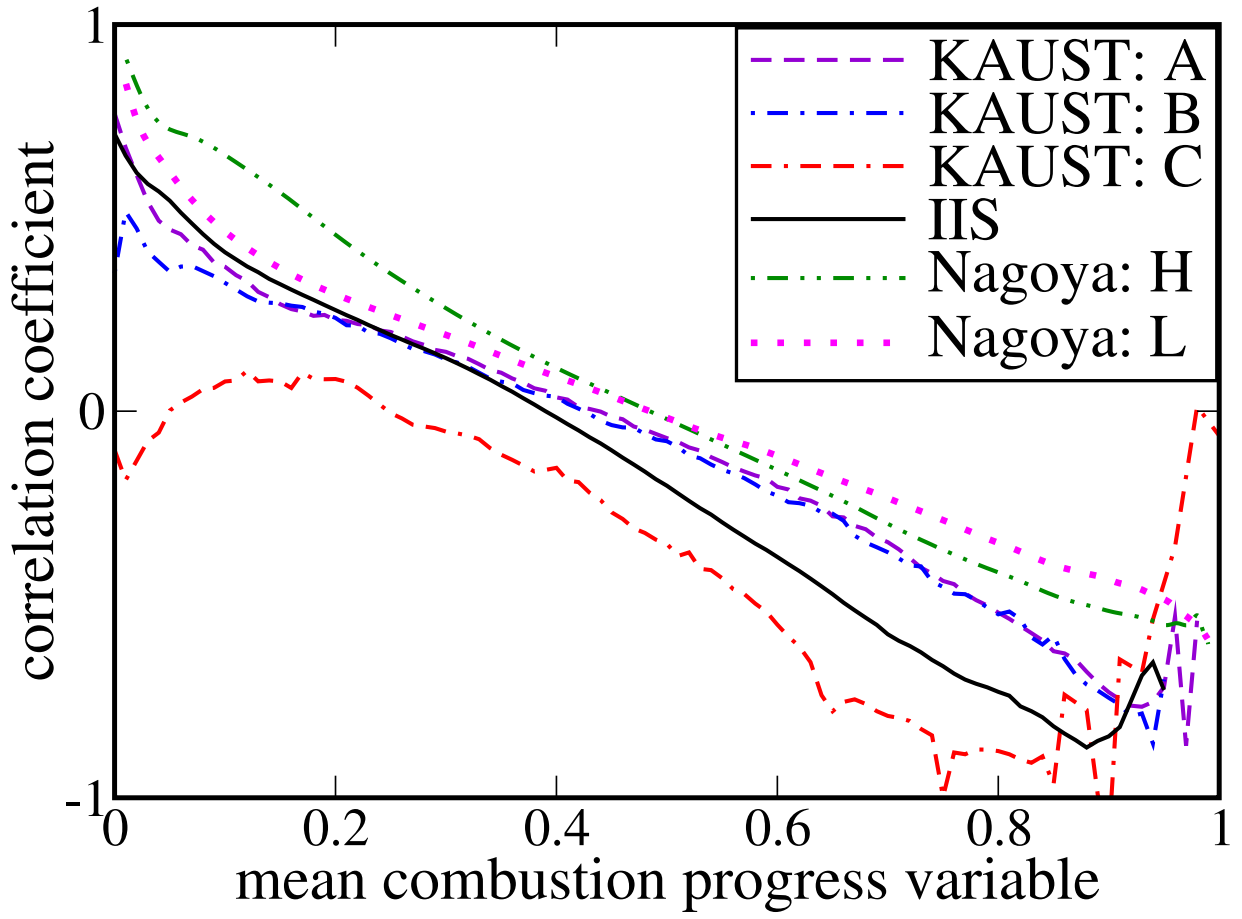
This is the author's peer reviewed, accepted manuscript. However, the online version of record will be different from this version once it has been copyedited and typeset.

PLEASE CITE THIS ARTICLE AS DOI: 10.1063/5.0039101

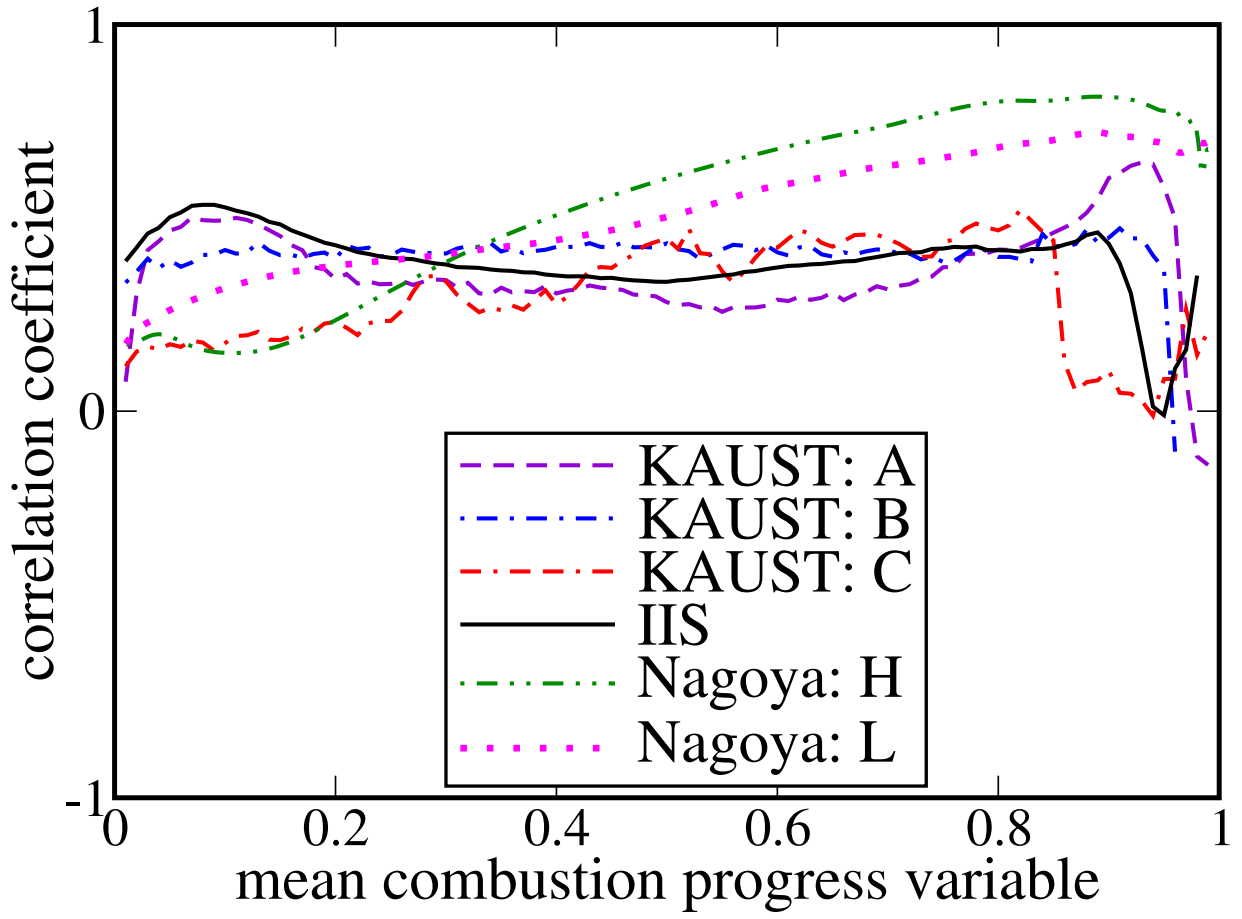


This is the author's peer reviewed, accepted manuscript. However, the online version of record will be different from this version once it has been copyedited and typeset.

PLEASE CITE THIS ARTICLE AS DOI: 10.1063/1.50039101

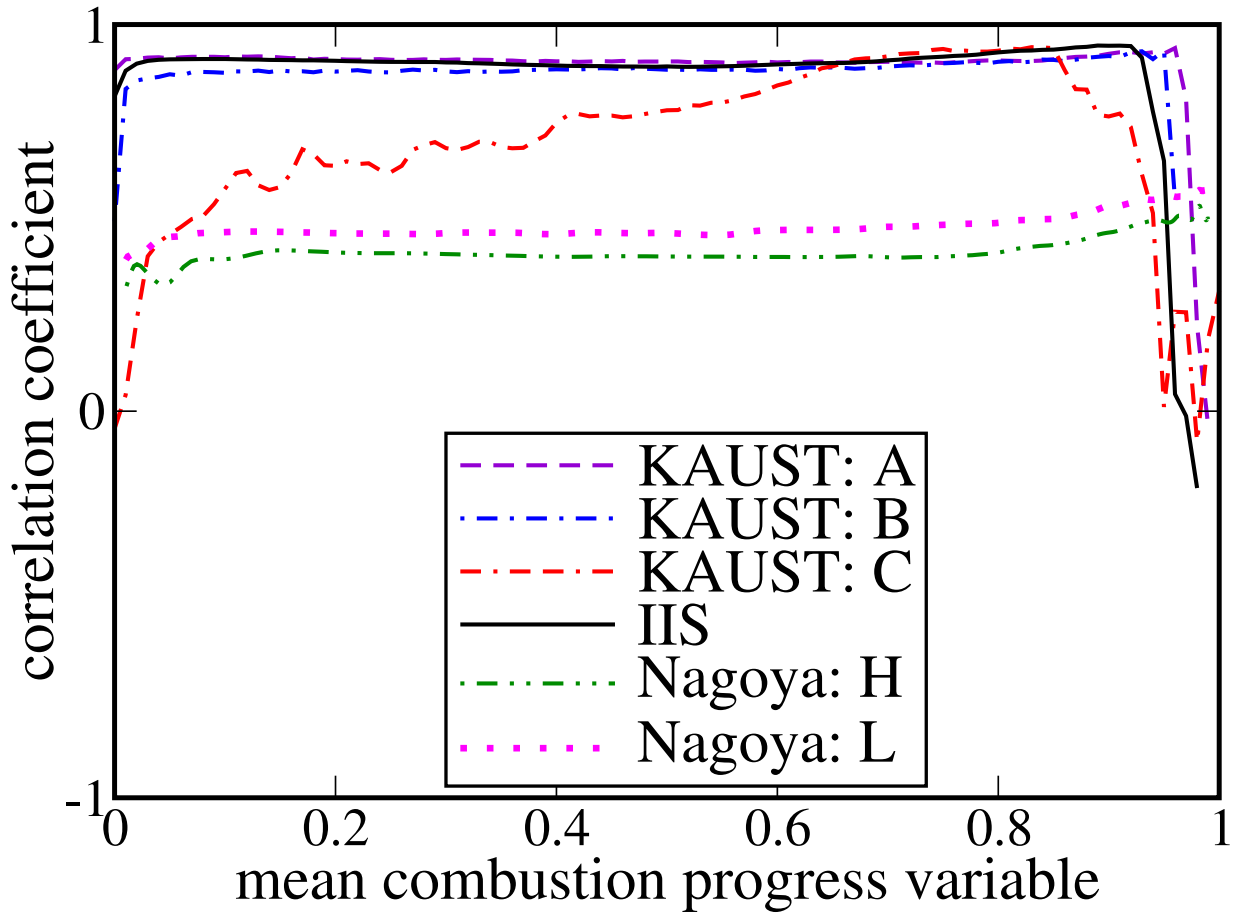


This is the author's peer reviewed, accepted manuscript. However, the online version of record will be different from this version once it has been copyedited and typeset.
PLEASE CITE THIS ARTICLE AS DOI: 10.1063/1.50039101



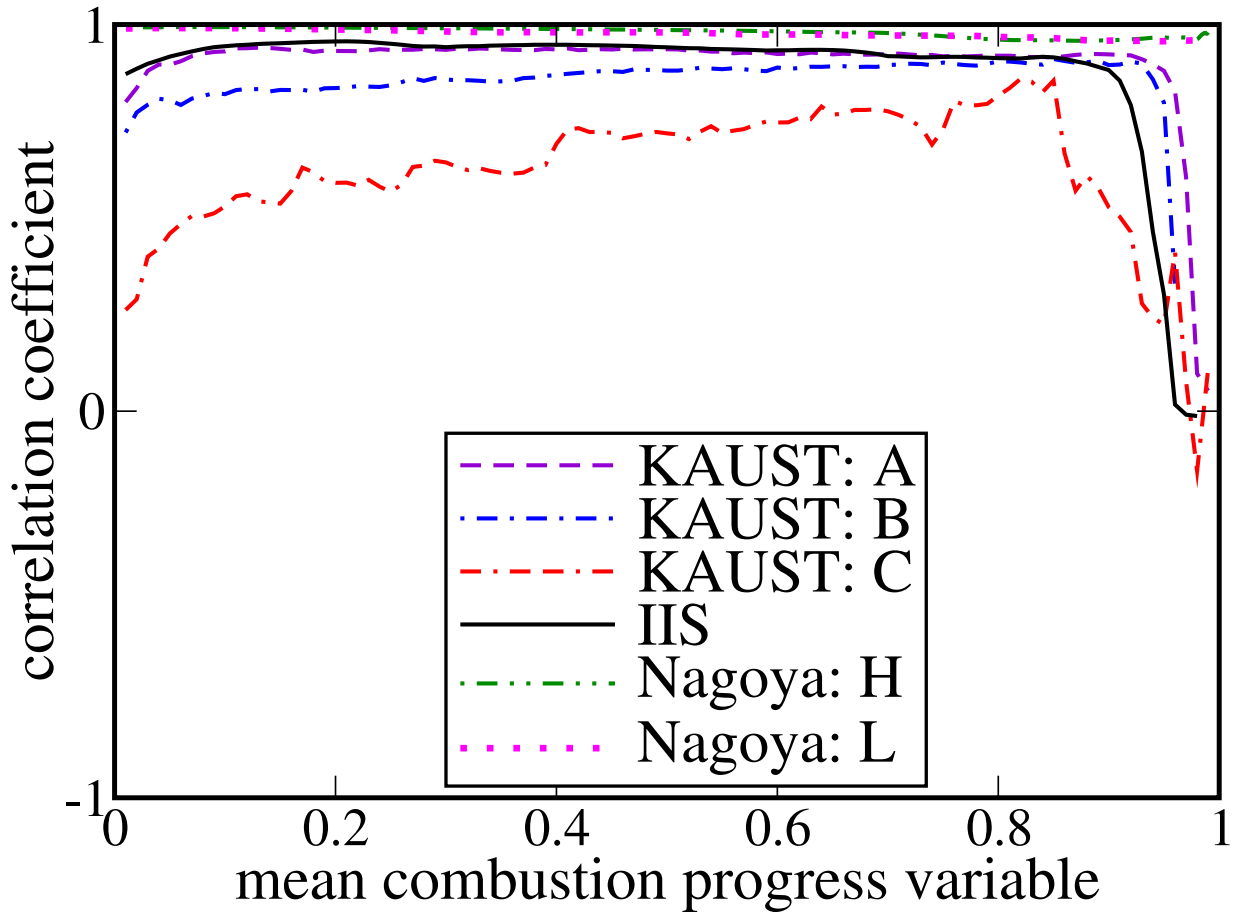
This is the author's peer reviewed, accepted manuscript. However, the online version of record will be different from this version once it has been copyedited and typeset.

PLEASE CITE THIS ARTICLE AS DOI: 10.1063/5.0039101



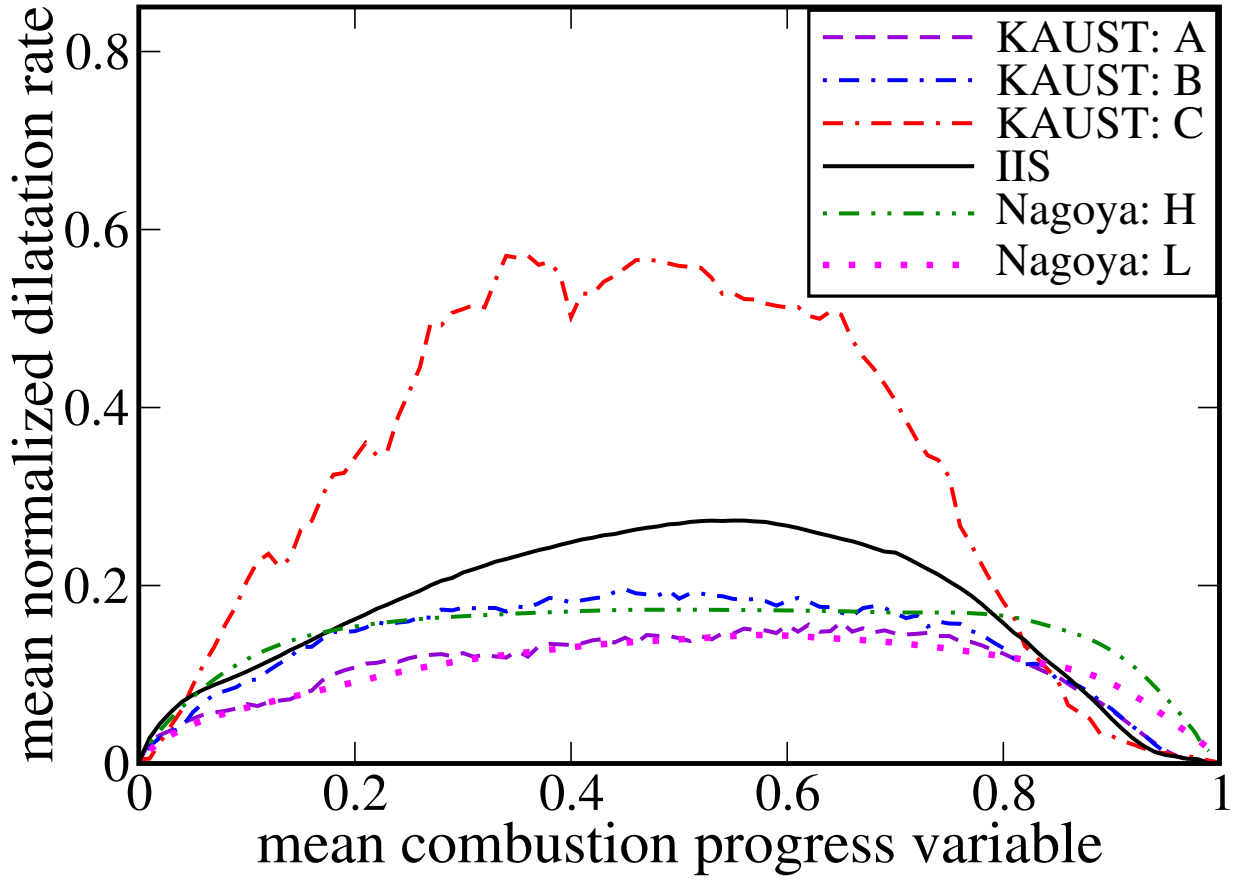
This is the author's peer reviewed, accepted manuscript. However, the online version of record will be different from this version once it has been copyedited and typeset.

PLEASE CITE THIS ARTICLE AS DOI: 10.1063/5.0039101

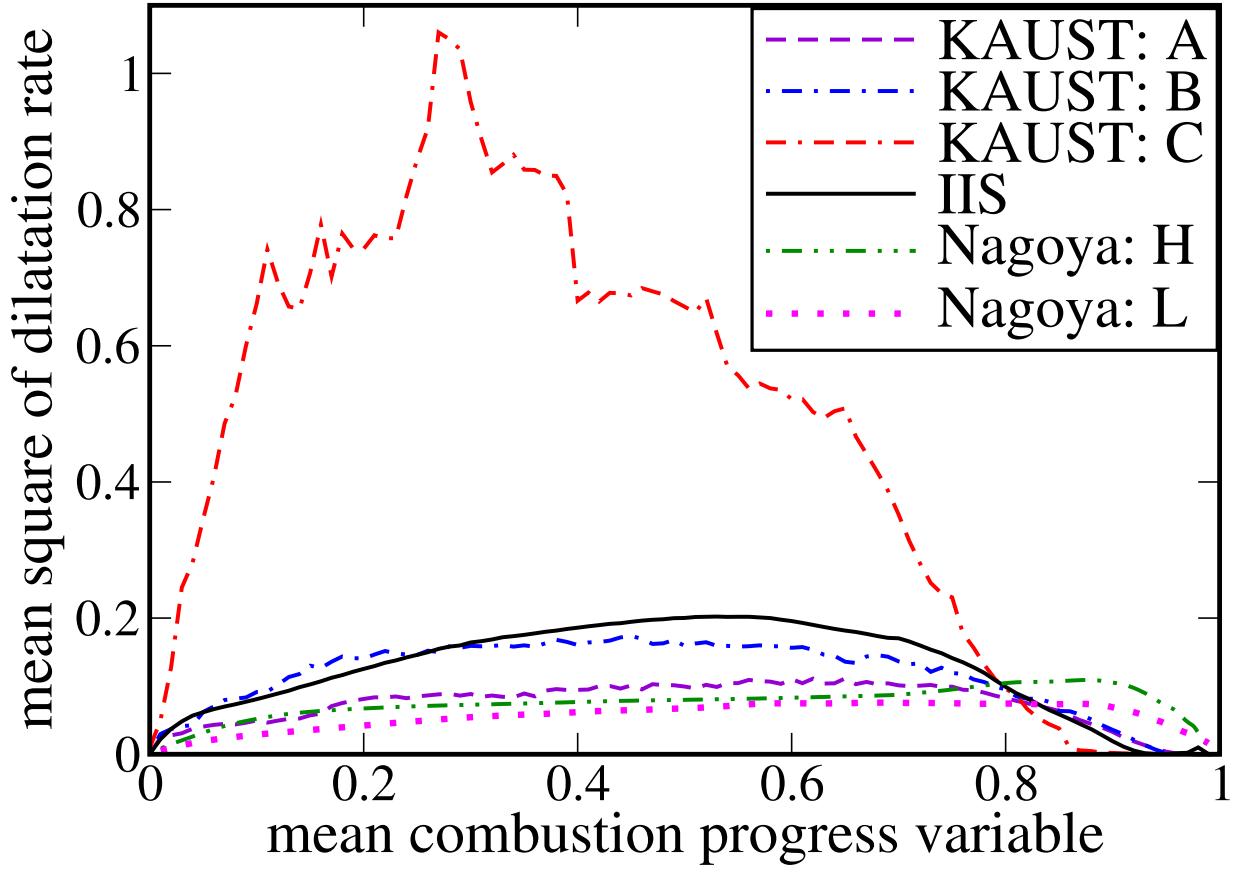


This is the author's peer reviewed, accepted manuscript. However, the online version of record will be different from this version once it has been copyedited and typeset.

PLEASE CITE THIS ARTICLE AS DOI: 10.1063/5.0039101

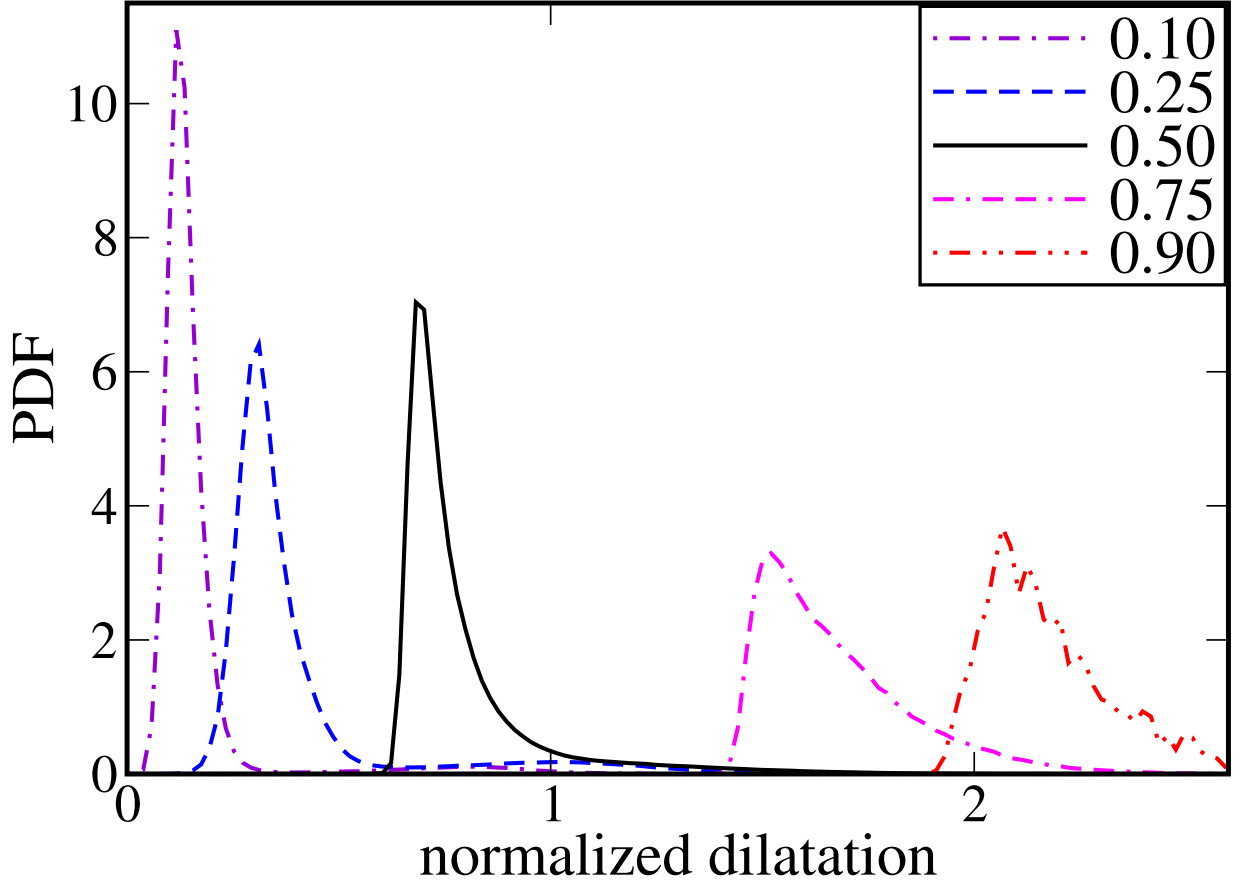


This is the author's peer reviewed, accepted manuscript. However, the online version of record will be different from this version once it has been copyedited and typeset.
 PLEASE CITE THIS ARTICLE AS DOI: 10.1063/1.50039101

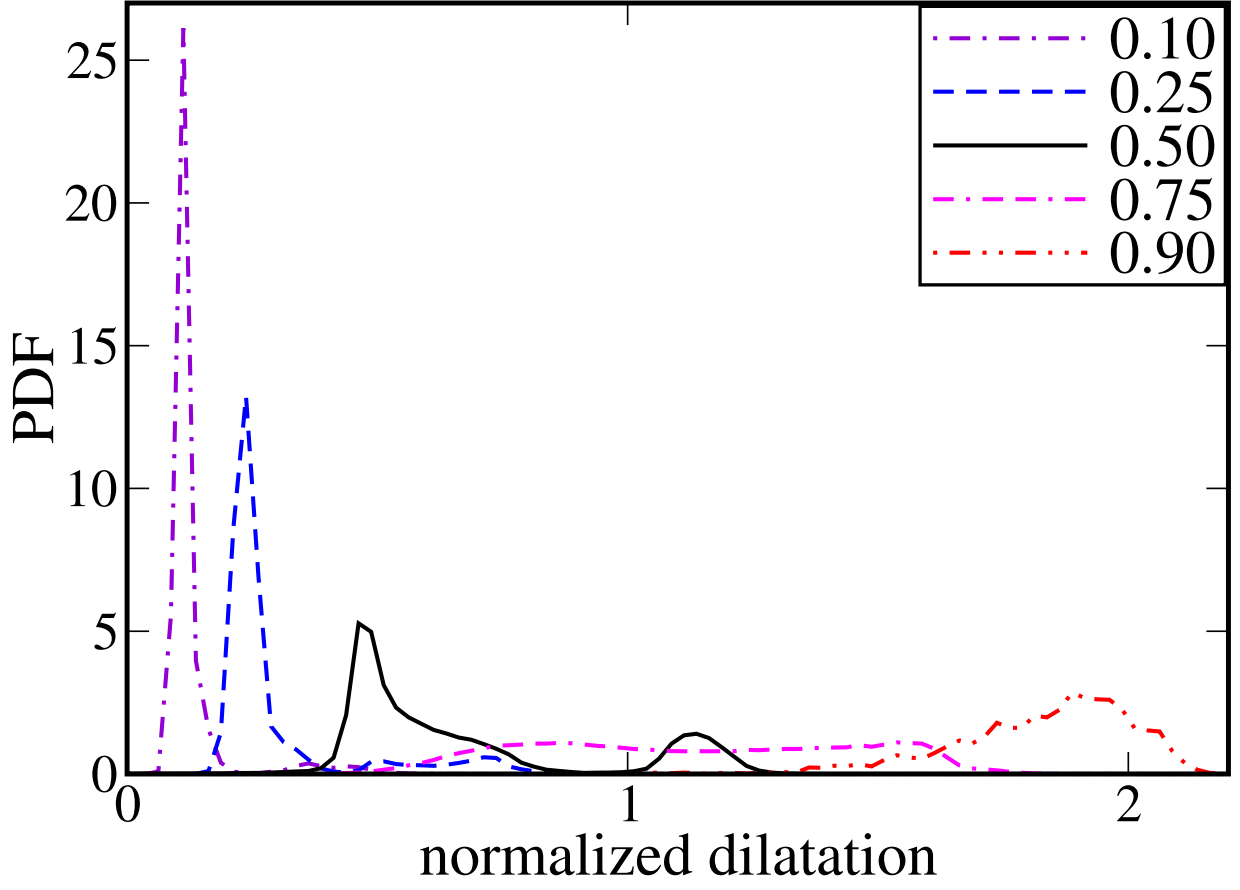


This is the author's peer reviewed, accepted manuscript. However, the online version of record will be different from this version once it has been copyedited and typeset.

PLEASE CITE THIS ARTICLE AS DOI: 10.1063/5.0039101

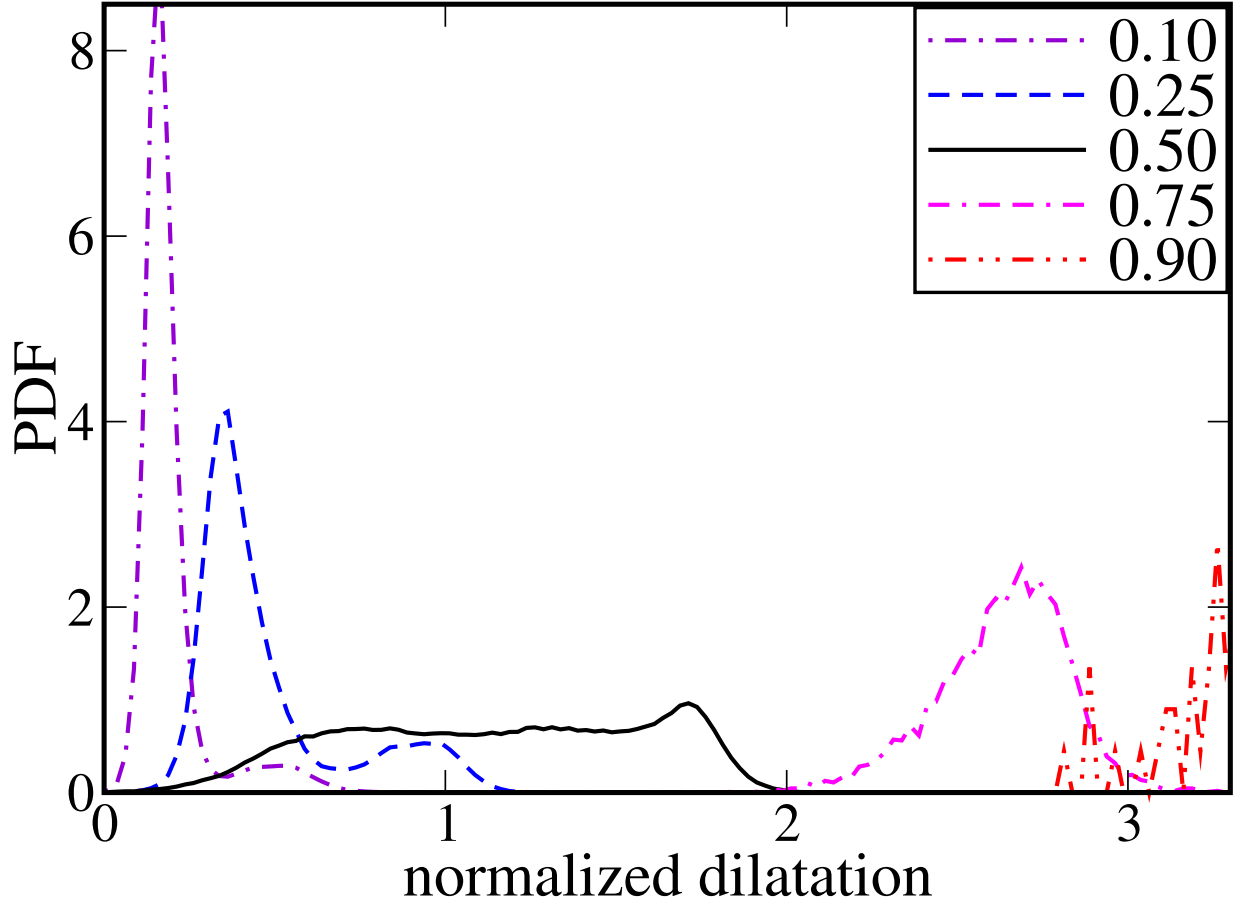


This is the author's peer reviewed, accepted manuscript. However, the online version of record will be different from this version once it has been copyedited and typeset.
 PLEASE CITE THIS ARTICLE AS DOI: 10.1063/1.50039101



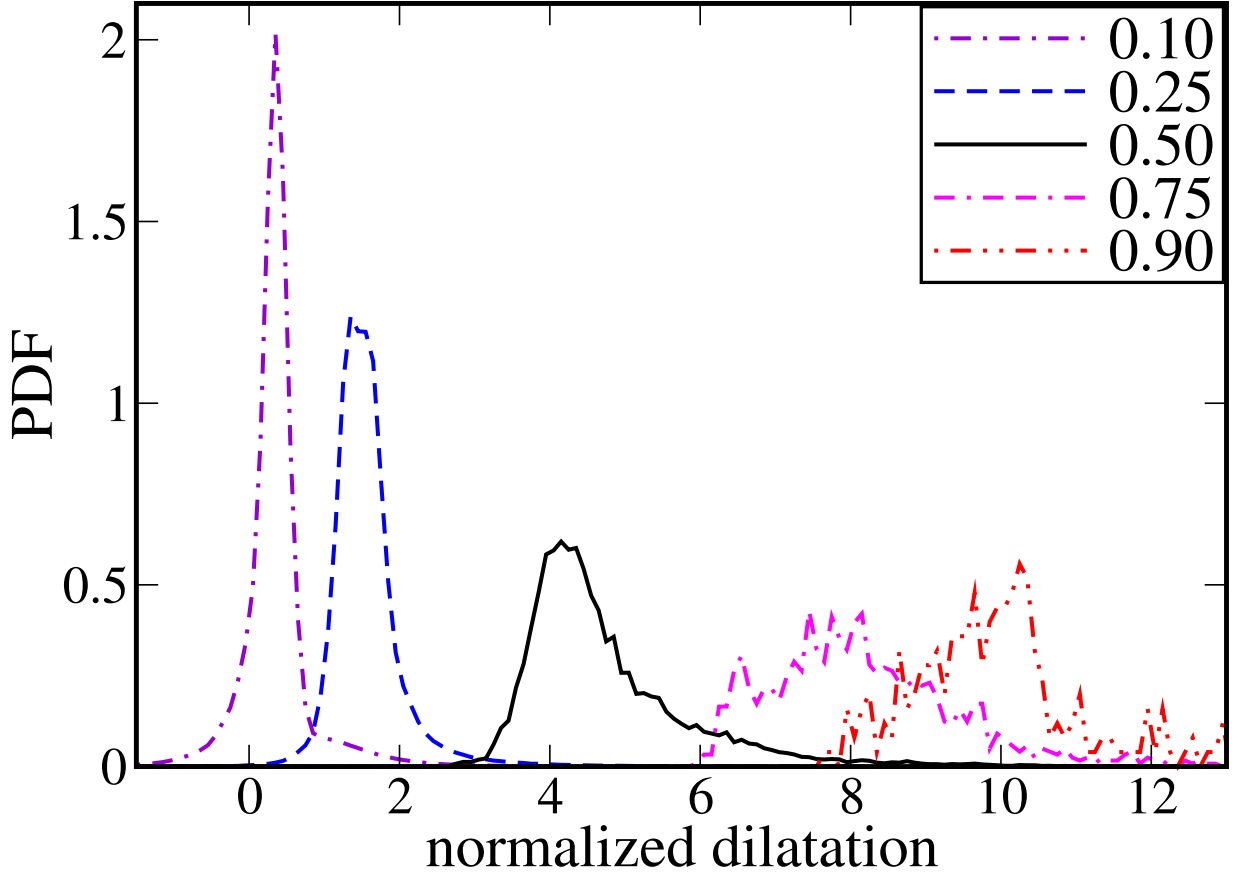
This is the author's peer reviewed, accepted manuscript. However, the online version of record will be different from this version once it has been copyedited and typeset.

PLEASE CITE THIS ARTICLE AS DOI: 10.1063/5.0039101



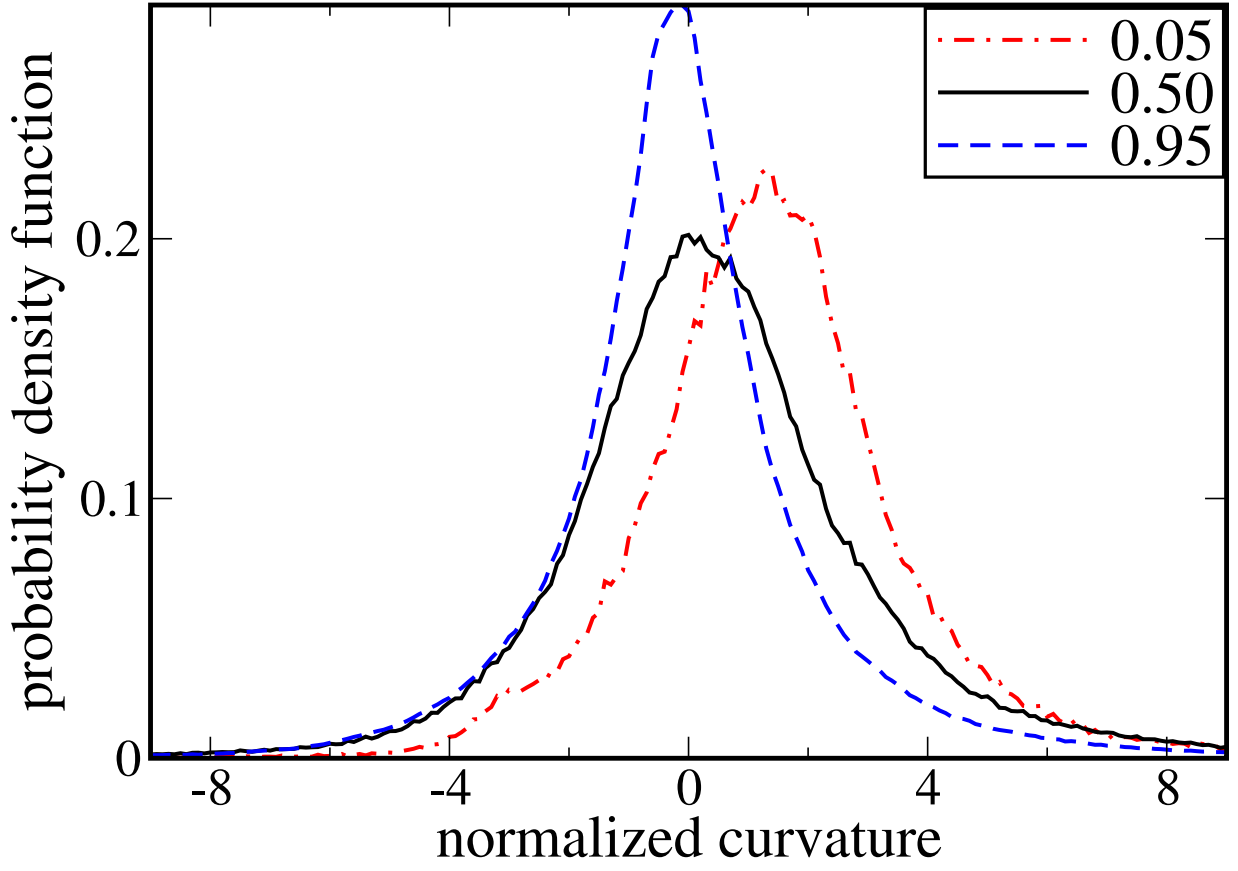
This is the author's peer reviewed, accepted manuscript. However, the online version of record will be different from this version once it has been copyedited and typeset.

PLEASE CITE THIS ARTICLE AS DOI: 10.1063/1.50039101



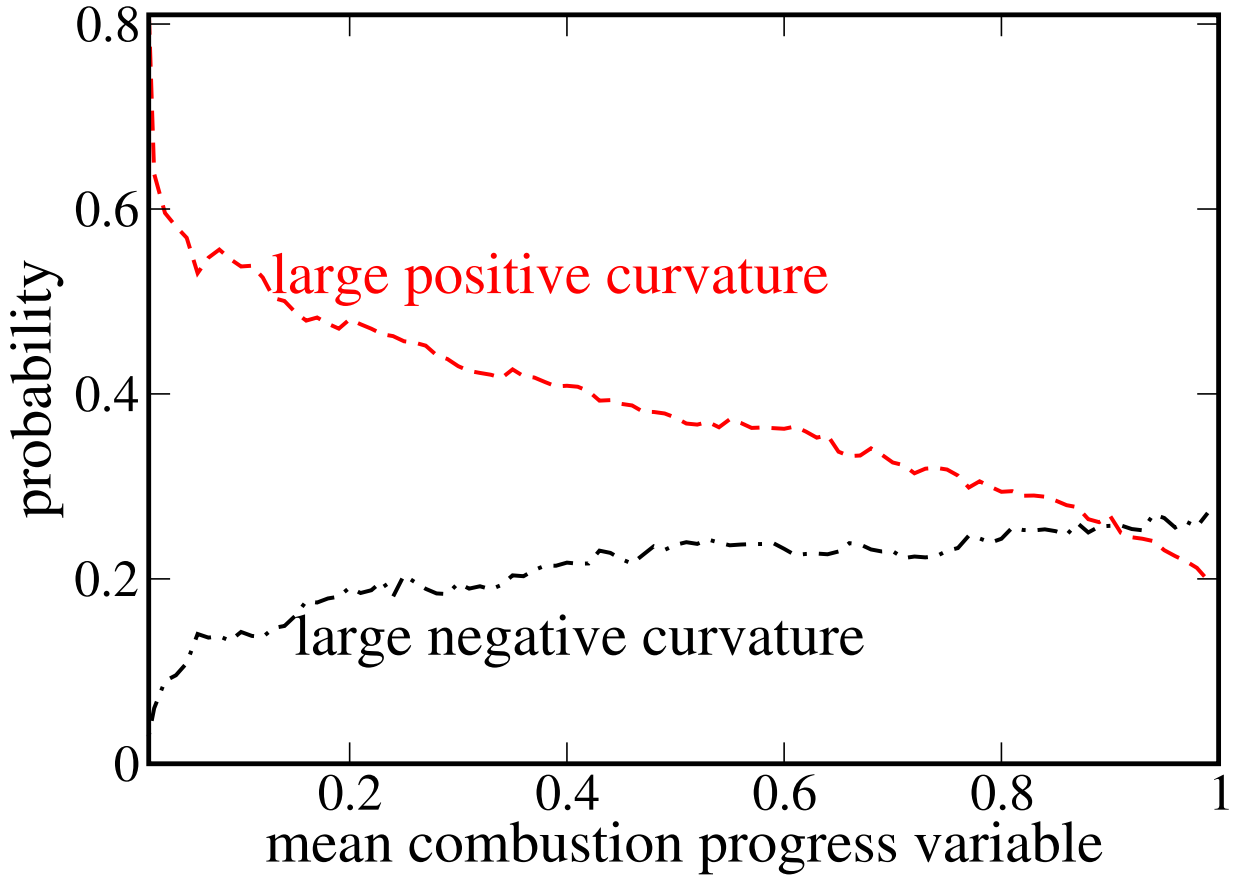
This is the author's peer reviewed, accepted manuscript. However, the online version of record will be different from this version once it has been copyedited and typeset.

PLEASE CITE THIS ARTICLE AS DOI: 10.1063/1.50039101



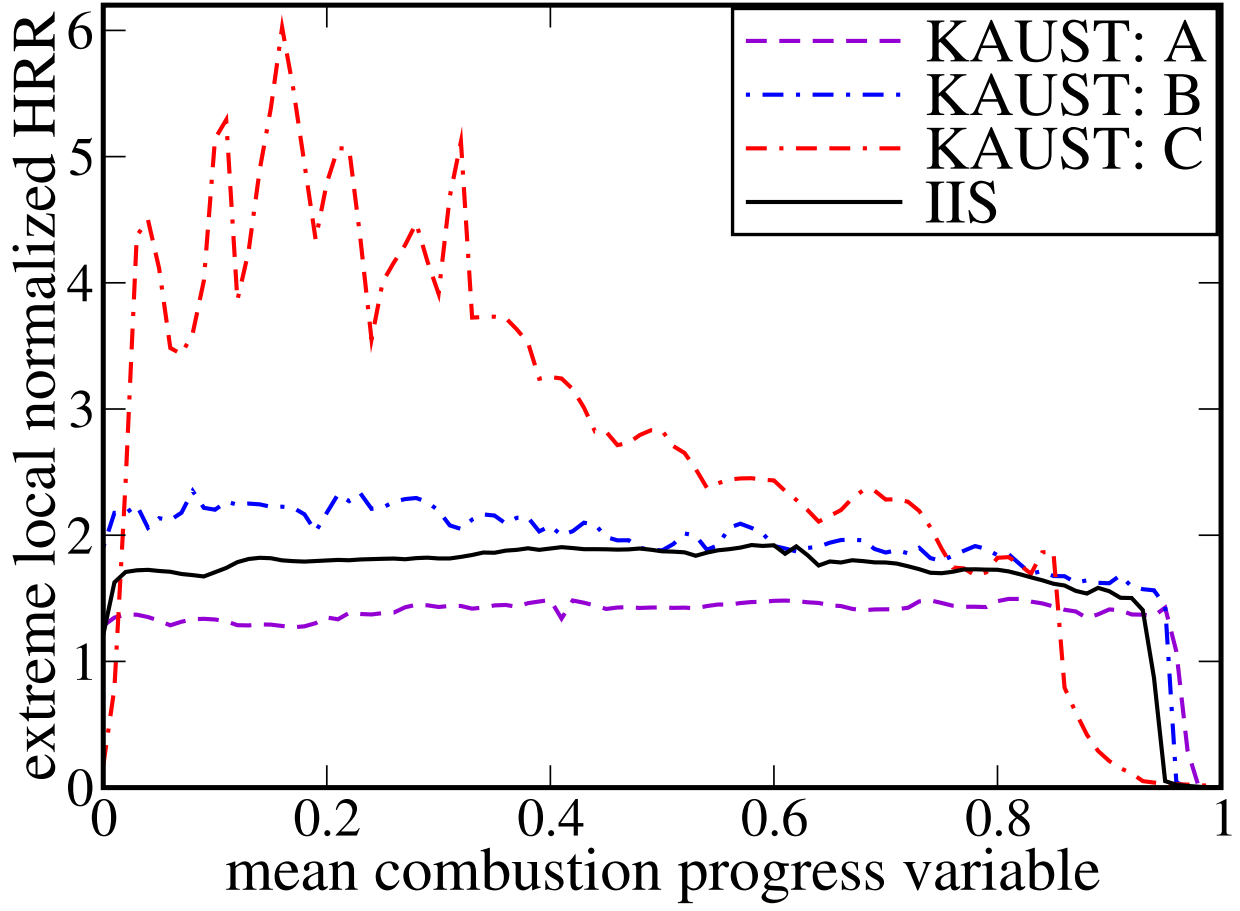
This is the author's peer reviewed, accepted manuscript. However, the online version of record will be different from this version once it has been copyedited and typeset.

PLEASE CITE THIS ARTICLE AS DOI: 10.1063/1.50039101



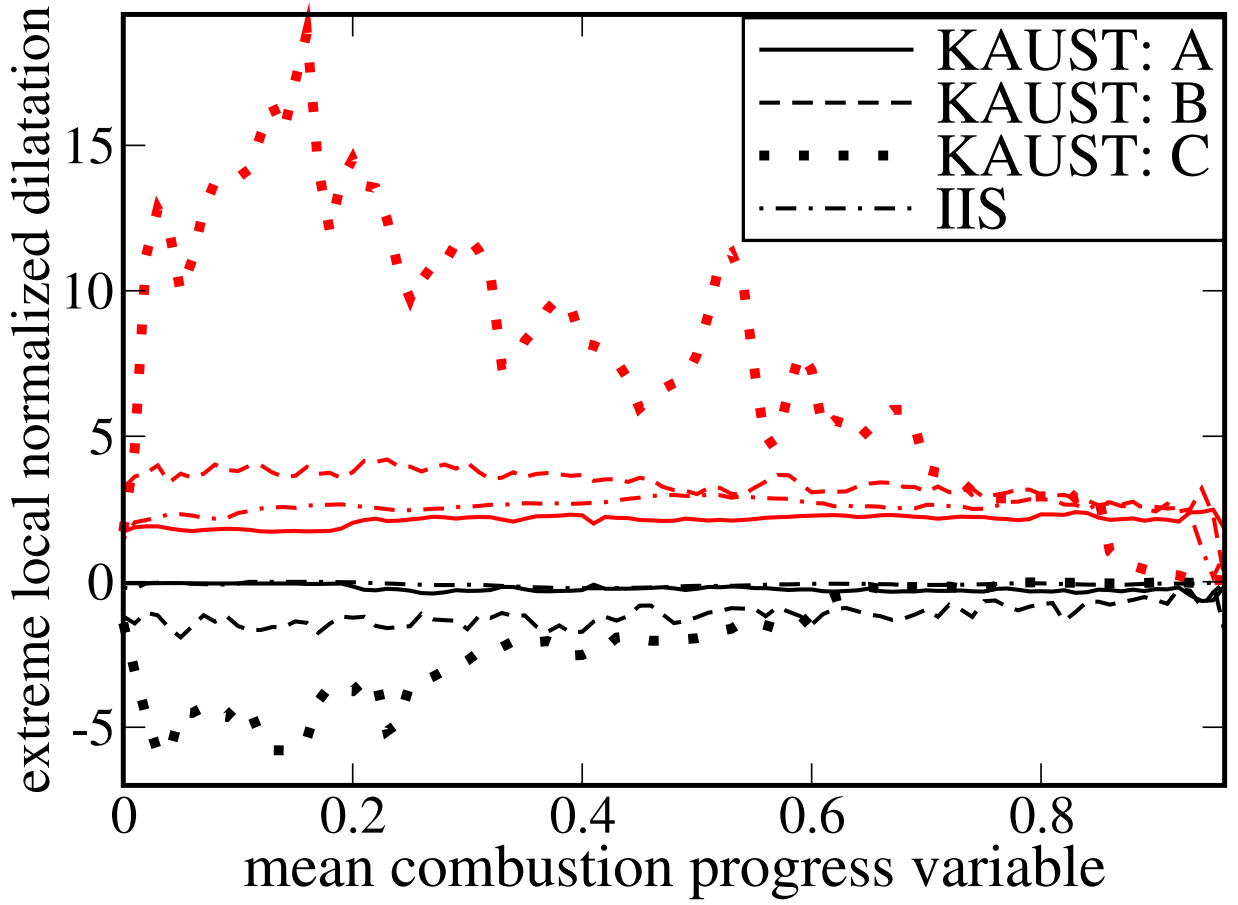
This is the author's peer reviewed, accepted manuscript. However, the online version of record will be different from this version once it has been copyedited and typeset.

PLEASE CITE THIS ARTICLE AS DOI: 10.1063/5.0039101



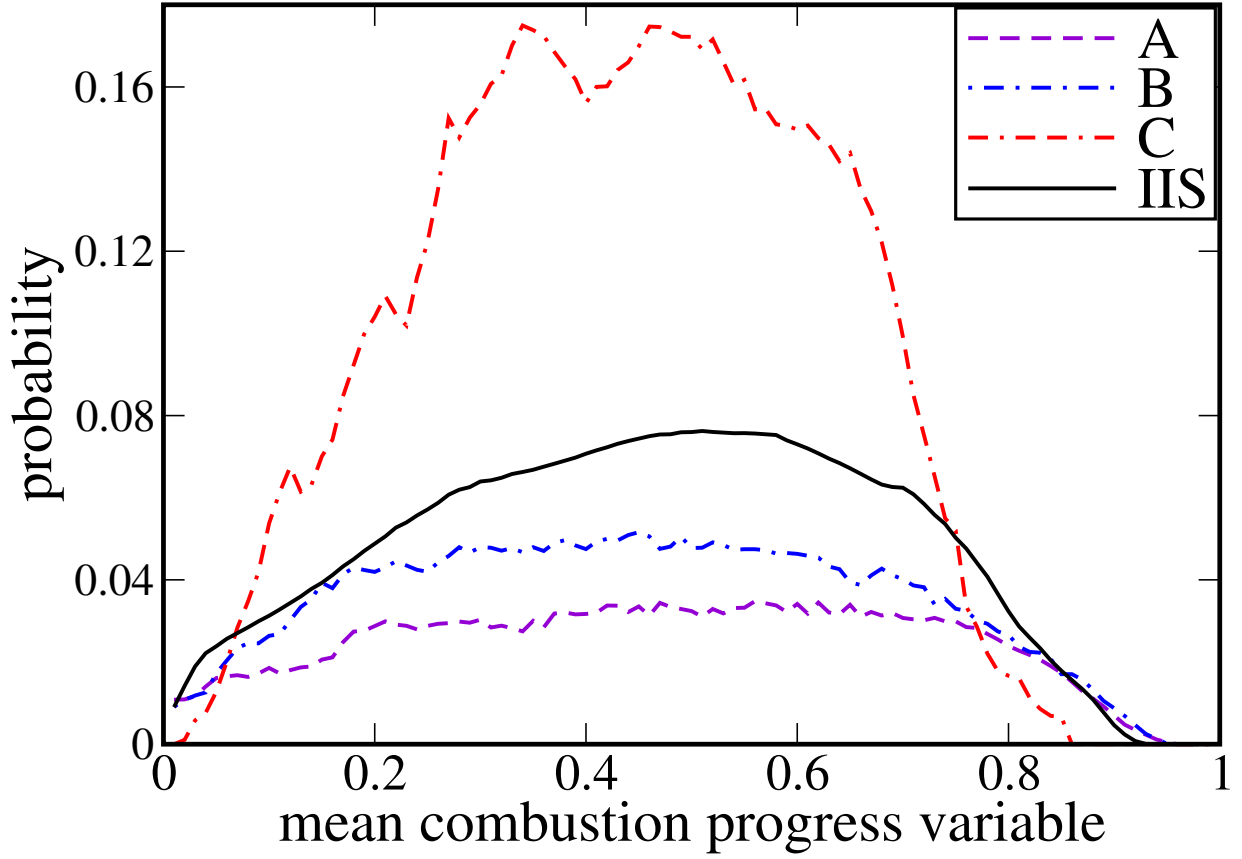
This is the author's peer reviewed, accepted manuscript. However, the online version of record will be different from this version once it has been copyedited and typeset.

PLEASE CITE THIS ARTICLE AS DOI: 10.1063/5.0039101



This is the author's peer reviewed, accepted manuscript. However, the online version of record will be different from this version once it has been copyedited and typeset.

PLEASE CITE THIS ARTICLE AS DOI: 10.1063/5.0039101



This is the author's peer reviewed, accepted manuscript. However, the online version of record will be different from this version once it has been copyedited and typeset.

PLEASE CITE THIS ARTICLE AS DOI: 10.1063/5.0039101

